Heliyon 10 (2024) e36143

Contents lists available at ScienceDirect

Heliyon

journal homepage: www.cell.com/heliyon

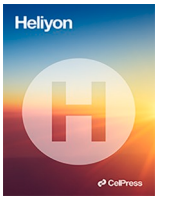

Review article

Current status and future trends of real-time imaging in gastric cancer surgery: A literature review

Zhu Liu [a,c,d,e], Muhammad Ali [b,d,e], Qiannan Sun [c,d,e], Qi Zhang [b,c,d,e], Chen Wei [b,d,e], Yong Wang [c,d,e], Dong Tang [b,c,d,e,**], Xin Li [c,f,*]

[a] The Yangzhou Clinical Medical College of Nanjing Medical University, Yangzhou, 225001, China
[b] Clinical Medical College, Yangzhou University, Yangzhou, 225001, China
[c] Northern Jiangsu People's Hospital, Yangzhou, 225001, China
[d] General Surgery Institute of Yangzhou, Yangzhou University, Yangzhou, 225001, China
[e] Yangzhou Key Laboratory of Basic and Clinical Transformation of Digestive and Metabolic Diseases, China
[f] Department of Pharmacy, Clinical Medical College, Yangzhou University, Northern Jiangsu People's Hospital, Yangzhou, China

A B S T R A C T

Technological advances are crucial for the optimization of gastric cancer surgery, and the success of any gastric cancer surgery is based on the correct and precise anatomical determination of the primary tumour and tissue structures. Real-time imaging-guided surgery is showing increasing potential and utility, mainly because it helps to aid intraoperative decision-making. However, intraoperative imaging faces many challenges in the field of gastric cancer. This article summarizes and discusses the following clinical applications of real-time optical imaging and fluorescence-guided surgery for gastric cancer: (1) the potential of quantitative fluorescence imaging in assessing tissue perfusion, (2) vascular navigation and determination of tumour margins, (3) the advantages and limitations of lymph node drainage assessment, and (4) identification of peritoneal metastases. In addition, preclinical study of tumour-targeted fluorescence imaging are discussed.

1. Overview of imaging-guided surgery

Gastric cancer is a global health problem: in 2020, there were approximately 1,089,103 newly diagnosed cases and 768,793 deaths worldwide [1]. Due to the late onset of symptoms, many gastric cancer (GC) patients are diagnosed at progression [2], and peritoneal metastases from GC still lack effective treatments. Multidisciplinary treatment pathways represent the standard of care for gastric cancer today, and radical surgery remains the cornerstone of resectable gastric cancer treatment [3]. Following laparoscopic and robotic techniques, intraoperative real-time imaging has made significant progress in the field of GC surgery. Image-guided surgery opens up new possibilities for intraoperative visualization of important surgical parameters such as tissue perfusion and lymphatic drainage.

Usually intraoperative differentiation of benign and malignant tissues is mainly based on tactile and visual examination by the surgeon. Both of these subjective methods have limitations in assessing tumour boundaries, metastatic lymph nodes, and as a result tiny tumour remnants or positive margins still occur frequently and can lead to local recurrence and metastasis [4]. One of the most significant advantages of image-guided surgical techniques is the ability to provide surgeons with real-time information that cannot be seen by the naked eye alone. This can be accomplished by utilizing the fluorescence intensity of the probe, which may fluoresce in

* Corresponding author. Department of Pharmacy, Clinical Medical College, Yangzhou University, Northern Jiangsu People's Hospital, Yangzhou, China.
** Corresponding author. General Surgery Institute of Yangzhou, Yangzhou University, Yangzhou, China.
E-mail addresses: 83392785@qq.com (D. Tang), 2292841764@qq.com (X. Li).

https://doi.org/10.1016/j.heliyon.2024.e36143
Received 8 March 2024; Received in revised form 23 July 2024; Accepted 9 August 2024
Available online 10 August 2024
2405-8440/© 2024 The Authors. Published by Elsevier Ltd. This is an open access article under the CC BY-NC license (http://creativecommons.org/licenses/by-nc/4.0/).

wavelength regions outside the visible spectrum, requiring a specialist camera, as well as by utilizing the fluorescence lifetime of the probe to provide additional contrast and environmental information at the location of interest [5]. This is largely attributed to the successful use of indocyanine green (ICG) in the evaluation of tissue perfusion [6–8]. The lack of selectivity and functionality of fluorescence navigation imaging has been a challenge, but in recent years a number of systems (e.g. fluorescent probe structures, imaging systems, and digitisation software) have been progressively improved this problem.

Intraoperative real-time imaging helps to improve some of the challenges of GC surgery, such as prediction of anastomotic leak, selective lymph node dissection, identification of variant vessels, determination of margins, and identification of peritoneal metastasis. In the last decade, although there were fewer clinical prospective randomized controlled studies on imaging-guided surgery for GC (Table 1), a number of new fluorescent probes, imaging systems, and comprehensive strategies have emerged. The aim of this review is to summarize some of the new opportunities and developments in imaging-guided surgery for GC that have emerged in recent years, as well as to highlight their advantages and the limitations that need to be overcome in order to fully utilize the potential of imaging-guided techniques in surgery.

2. Perfusion fluorescence imaging

Anastomotic leak is one of the most serious postoperative complications in GC surgery, with a reported incidence of 0–17 % and a mean incidence of 5–8% [9]. After reconstruction of the digestive tract, judgement of tissue colour and vascular pulsation is made under standard light and leakage tests, a conventional method that relies on subjective experience of the surgeon. Karliczek et al. argued that empirical intraoperative evaluations by the surgeon are very subjective and unreliable because they have very low sensitivity and specificity [10]. Whereas the intraoperative methylene blue leak detection may be useful for identifying suture rupture, it is not applicable for identifying increased risk of subsequent leakage [11]. In order to assess intraoperative anastomotic perfusion more objectively and accurately, several studies have demonstrated the validity of polarographic oxygen tonometry, laser Doppler flow measurement, or Doppler ultrasound for the assessment of anastomotic leaks. However, the results of the above studies remain

Table 1
Clinical trials of fluorescence imaging for gastric cancer surgery.

Authors	Journals	Research Methods	Number of Cases	Fluorescent Agent	Imaging System	Main Results
Chang-ming Huang [118]	International Journal of Surgery, 2021	Prospective, Randomized controlled trial	514	ICG	NOVADAQ fluorescence surgical system (Stryker Corp., Kalamazoo, MI, USA)	1. Selective fluorescence station lymph node dissection is recommended for patients with cT1-cT2 gastric cancer. 2. Systematic fluorescence imaging-guided lymph node dissection is recommended for patients with cT3-cT4a gastric cancer.
Chang-ming Huang [119] (FUGES-019)	BMC Medicine, 2021	Prospective, Randomized controlled trial	259	ICG	NOVADAQ fluorescence surgical system (Stryker Corp., Kalamazoo, MI, USA)	1. Intraoperative ICG administered by subserosal injection was comparable to that administered by submucosal injection for lymph node tracing in gastric cancer. 2. Intraoperative subserosal injection is a more reasonable choice: good patient satisfaction and cost-effective.
Vincenzo Mazzaferro [120]	Ann Surg Oncol, 2023	Single-arm, simon's two-stage, adaptive, phase II trial	18	ICG	NOVADAQ SPY Elite system (Stryker®)	1. ICG-Fluorescent Navigation Surgery may improve the quality of lymph node dissection without causing harm. 2. The real benefit of additional NIR-induced lymph node dissection seems to be limited.
Quirijn RJG Tummers [121]	World J Gastroenterol, 2016	Single-arm trail	22	ICG: Nanocoll	Mini-FLARETM image-guided surgery system	1. Excellent examination accuracy was observed in T1 and T2 gastric tumours with ICG combined with nanocolloids. 2. Tumour positive lymph nodes outside the standard anatomical plane can be identified.
Chang-ming Huang [74] (FUGES-012)	JAMA Surgery, 2022	Prospective, Randomized controlled trial	266	ICG	NOVADAQ fluorescence surgical system (Stryker Corp., Kalamazoo, MI, USA)	ICG-guided laparoscopic radical gastrectomy for gastric cancer harvests more lymph nodes and reduces lymph node non-compliance, especially in patients undergoing total gastrectomy.

ICG:Indocyanine Green

Table 2
Fluorescence imaging method for assessing anastomotic leak after gastrectomy.

References	Type of Research (Number of Cases)	ICG Dose	Surgical Method	Imaging System	The Main Measurement	Evaluation Criteria
Visual Fluorescence Imaging Assessment						
Brian, 2017 [28]	Prospective clinical study (40)	7.5 mg	E-G	PINPOINT	Presence of perfusion demarcation in the gastric wall	No perfusion demarcation seen within 60 s of injection
Noma K, 2018 [26]	Retrospective clinical study (285)	12.5 mg	E-G	NIR	The time to visible perfusion of the gastric wall after ICG injection	No fluorescence for more than 30 s
Kumagai Y, 2018 [24]	Clinical cohort study (18)	2.5 mg	E-G	PDE	Time of visible fluorescence at the root of the right omental artery after ICG injection	No fluorescence for more than 90 s
Elke Van Daele 2022 [30]	Retrospective clinical studies (266)	0.5 mg/kg	EG	NIR	1.Fluorescence development time 2.Fluorescence homogeneity	The results were not statistically different
Slooter, 2021 [29]	Prospective clinical study (84)	0.05 mg/kg	E-G	PINPOINT	1.Time from ICG injection to fundus imaging 2.Time from ICG injection toanastomosis imaging	The results were not statistically different
Yeon-Ju Huh, 2018 [21]	Prospective clinical study (30)	2.5 mg	DG, TG, PPG	NIR	The Sherwinter scale	The results were not statistically different
Quantitative Fluorescence Imaging Assessment						
Haryadi Prasetya, 2019 [38]	Preclinical studies	–	Tube gastric model	–	Pass Threshold Relative Time (RTT) Predicting Relative Residual Flow (RRF)	RTT less than 20 % of the maximum threshold
Nikolaj Nerup, 2020 [31]	Prospective clinical study (10)	0.5 mg/kg	E-G	Image-1 SPIES (software)	1.slope of the curve (Δfluorescence intensi ty/Δtime) 2.relative values of perfusion (slope/max slope)	–
Jens Osterkamp, 2020 [41]	Preclinical studies (10 animal models)	0.25 mg/kg	E-G	PINPOINT	Normalized slope	–
Philipp von Kroge, 2021 [34]	Clinical cohort study (20)	0.02 mg/kg	E-G	SPY Elite; MVCL (software)	SFI, BSFI, TTS	SFI reduction of >32 %, BSFI reduction of >23 %
Sanne M. Jansen, 2022 [37]	Clinical cohort study (22)	–	E-G	NIR	FImax, Tmax, Fslope	Fslope <0.2
Koyanagi, 2016 [22]	Clinical cohort study (40)	–	E-G	PDE	Flow rate of ICG through the gastric wall	ICG flow rate <1.76 cm/s
Mikito Mori, 2020 [39]	Retrospective clinical study (100)	0.5 mg/kg	B–I/B-II/ RY/EG	Image-1 SPIES	DT, ST	ST ≥ 34s, DT ≥ 18 s
Kazuo Koyanagi, 2020 [23]	Prospective clinical study (109)	1.25 mg	EG	PDE	Flow rate of ICG	Fluorescent blood flow velocity ≤2.07 cm/s in the lateral gastric lesser curvature
Anna Dupre'e, 2020 [42]	Preclinical studies (7 animal models)	0.02 mg/kg	E-G	LLS GmbH (software)	SFI, BSFI, TTS	–

PDE:Photo dynamic Eye. EG:esophagogastrostomy; DG:distal gastrectomy. TG:total gastrectomy. PPG: Pylorus preserving gastrectomy. MVCLF : Meteroarchive VCL LLS Fluoreszenzangiographie V 1.0.

controversial, and the application of these techniques in minimally invasive surgery requires further research [12]. Another line of research suggest that the intensity of the NIR fluorescent signal detected from the tissue after intravenous injection of a fluorophore can be used as a marker of tissue perfusion. Another major advantage of this method is the ability to repeatedly inject fluorescent agents (e.g., ICG), which may allow anastomotic revision if poor anastomotic perfusion is detected [13,14].

There are no uniform and standardized parameters for the evaluation of anastomotic perfusion. A study by Hardy NP demonstrated that there is significant variability in the interpretation and practice of fluorescence imaging angiography (ICGFA), and the results remain limited by the subjective level and proficiency of the evaluator [15]. Current software-based quantitative vascular perfusion imaging overcomes the variability in subjective evaluation to some extent. Table 2 summarizes a number of preclinical or clinical studies that have examined different methods to assess anastomotic perfusion.

2.1. Visual fluorescence imaging (v-FI)

The fluorescence spectrum of ICG is in the near-infrared range and can be captured by a specialized camera after illumination of the tissue of interest. Because of the high plasma disappearance rate of ICG, deviations in the fluorescence signal can be used to represent tissue perfusion, and it is currently the most widely used fluorescent agent in surgery. However, ICGFA is a visual assessment based on fluorescence images captured by the camera, and the output is limited to binary ratings, i.e. perfused or nonperfused tissue [16,17]. Kazuo Koyanagi retrospectively found that all seven patients presenting with anastomotic leaks were successfully fluorescently

Table 3
Optical techniques for perfusion monitoring of the gastric wall after gastrectomy.

Methods	Optical Principle	Evaluation Unit	Physiological Evaluation	Depth of Imaging	Demand for Fluorescent	Vantages	Drawbacks	Future Prospects
LSCI	Laser scattering pattern	Laser Spot Perfusion Unit (LSPU)	Scatter contrast inversely proportional to flow rate	700–1000 μm	No	1. Continuous and real-time assessment 2. Combining with ICG for physiologic imaging 3. Spatio-temporal precision and accuracy	1. Evaluation limited to the serosal layer 2. High angle and space requirements	Exploring applications in minimally invasive surgery
TI	Temperature of the tissue surface	Anastomotic Viability Index (AVI)	AVI = L-GEA[a] × TRr[a](AVI ≤0.61 suggests high leak risk)	2000 μm	No	1. Direct measurement of blood flow distribution 2. Repeatable measurement 3. Suitable for minimally invasive surgery	1. Only still photos can be observed 2. Inability to clearly visualize vascular structures 3. Narrow application scope, requiring frequent algorithm changes	Software development and algorithm expansion are needed to broaden the scope of suitable surgical applications
HSI	Analysis of light interactions (absorption, reflection) on tissue surfaces, reflecting various intrinsic biochemical properties of the tissue.	oxygen saturation (StO_2), near-infrared perfusion index (NIR), hemoglobin index (THI), and tissue water index (TWI) et al.	StO_2 in HSI dataset reflects tissue perfusion	6 mm	No	1. Providing rich and fine spectral characterization 2. Simultaneous provision of two-dimensional spatial information 3. Complementary advantages with fluorescence imaging 4. Repeatable observations 5. Easy selection of areas of interest	1. Still images only 2. Inability to provide information in small spaces (meaning difficult to assess after reconstruction) 3. Lack of real biological parameters to confirm the accuracy of HSI	1. Translating HSI technology into virtual reality, and Visualization of spatial data 2. Minimally invasive HSI
LDH & VLS	Laser, Doppler shift and the absorption spectra	rHb[a] , StO_2	Decrease in StO2 and increase in rHb, reflecting inadequate tissue perfusion and increased venous venous congestion	500 μm	No	1. Fast, less invasive and highly reproducible. 2. Measurements are done through microcatheters, suitable for laparoscopic surgery. 3. Easy operation	1. Need for quantitative values from a wider range of samples to improve reliability 2. Tissue structure and perfusion cannot be visualized	Results from a large number of more extensive studies are needed to standardize the way microcirculation is assessed for clinical use.

[a] L-GEA:length ratio of the gastroepiploic artery. TRr: temperature retain rate. rHb:relative hemoglobin amount.

visualized around the anastomosis by the naked eye during the operation [22]. A prospective study included 100 patients by Eider Talavera-Urquijo demonstrated [18] that subjective perfusion assessment was a very specific monitoring method (94.1 %) with a good negative predictive value (NPV 71.9 %, $p = 0.034$), but was insufficient to detect patients at risk of leakage (low sensitivity 21.8 %, positive predictive value 63.6 %). Niall P. Hardy reviewed eight patients undergoing laparoscopic surgery and invited experts to assess surgical video by questionnaire. They found that the interpretation of ICGFA and the resulting effects varied considerably between observers, and even skilled users may encounter challenges in particular situations [19]. Therefore, visual-dependent, two-dimensional, and subjective evaluation methods have significant shortcomings. Nevertheless, some studies have explored and optimized some visual qualitative data to assess anastomotic perfusion.

Table 4
SWOT analysis of lymph node navigation surgery.

Strengths	Weaknesses
1. Considerable number of clinical trials	1.Controversy surrounds whether there is a survival benefit for progressive gastric cancer
2. Selective lymph node dissection, preservation of function	2.Non-tumour specific fluorescence, fluorescence is usually greater than the area of the sentinel lymph node
3. ICG is easy to apply and has low side effects	3.Metastatic lymph node acquisition rates do not appear to be increasing
4. A broad perspective for fluoroscopy-guided surgery/ laparoscopic systems	4.High rate of false negatives in anterior lymph nodes
5. High lymph node test count	5.Difficulties in recognition after neoadjuvant therapy
Opportunities	Threats
1. Selective lymph node dissection for early gastric cancer (D1/D1+)	1.Differences in results between frozen pathology sections and permanent sections limit the accuracy of the extent of surgical excision
2. Additional surgery after ESD can also be beneficial	2.Long learning curve
3. The concept of "lymph basin dissection" instead of "anterior lymph node dissection"	3.ICG extra-cavity leakage, contaminating the operative area
4. Three-dimensional simulation technology	4.Specific probes to track gastric lymph nodes are questionable and lack preclinical/clinical studies, are expensive and have unproven safety
5. Development of quantitative ICG software	5.Other non-specific tracers are not superior to ICG and are expensive

2.1.1. Anastomotic perfusion rating scale: easy to use but with limitations

Earlier studies have explored the pitfalls of visual assessment of perfusion. In the 2013, D.A.Sherwinter observed angiographic as well as mucosal perfusion in 20 patients undergoing low anterior resection of the rectum [20], and proposed an anastomotic perfusion scale. The Sherwinter scale evaluates anastomotic perfusion based on two dimensions: clinical information (colour of the anastomosis, whether bleeding occurs, and the intensity of the anastomotic vessels) and fluorescence images (including homogeneity and intensity) with a score of 1–5 for each dimension. In a prospective study of 30 gastric resections by Yeon-Ju Huh [21], the Sherwinter scale was followed to evaluate intraoperative anastomotic perfusion of the distal gastrectomy (DG), total gastrectomy (TG), and pylorus preserving gastrectomy (PPG). Due to the small sample size, only one anastomotic leak (1/30) was observed, but this anastomotic leak had a clinical score of 5 and a fluorescence score of 4. In addition, there was a high incidence (5/30) of ICG imaging failures (perfusion scores less than 2 at more than two anastomotic sites), all of which were seen in distal gastrectomies, yet no evidence of anastomotic leak was observed in any of these patients. The Sherwinter scale is still limited by qualitative evaluation methods and has not been widely accepted.

2.1.2. Blood flow rate or development time: possible predictors of anastomotic leak

In some earlier studies, experts found that the occurrence of anastomotic leak risk was predicted by ICG measurements of peri-residual gastric blood flow velocities. Kazuo Koyanagi first proposed a new method to assess ICG fluorescence blood flow in the wall of the gastric conduit during oesophagectomy in 2016 [22], and anastomotic leak were significantly higher in patients with perigastric vascular flow velocities (1.8 ± 0.4 cm/s) lagging behind gastric wall fluorescence imaging, compared with those with perigastric vascular flow velocities (3.5 ± 1.3 cm/s) synchronized with the gastric wall ($p < 0.001$). Perigastric blood flow velocity was an independent risk factor for anastomotic leak, and a cut-off value of 1.76 cm/s (AUC = 0.96) was determined for the flow velocity of ICG fluorescence across the gastric tube wall. Similarly, a prospective study examined the relationship between fluorescence site, vascular fluorescence flow velocity and the risk of anastomotic leak in oesophagogastric anastomosis. The study selected 109 patients with gastroesophageal anastomosis and found that fluorescence flow velocity on the lesser curvature side of the gastric wall had a greater effect on anastomotic leak than on the greater curvature side, and ICG fluorescence flow velocity less than 2.07 cm/s ($p < 0.001$), as well as calcification of the superior mesenteric artery ($p = 0.026$), were independent risk factors for gastroesophageal anastomotic leaks [23].

Considering the complexity of determining blood flow velocity, there may be value in calculating the fluorescence development time of the gastric wall after ICG injection. Kumagai Y pioneered the 90-s principle in 2018, whereby reconstructed blood flow is adequate if anastomosis is performed in an area where ICG fluorescence angiography is demonstrated in less than 60 s, whereas insufficient blood supply to the residual stomach can be avoided if areas with imaging times longer than 90 s are resected [24]. Similar studies have indicated that perfusion times of more than 60 s suggest inadequate perfusion [25]. A recent report by Noma [26] compared the results of 285 patients before and after ICG injection. If fluorescent perfusion is visible in the anastomosis within 20 s, anastomosis is performed in that area, and if perfusion is seen within 30 s, some tissues should be freed to reduce tension or the staples may be removed for manual suturing. Whereas if fluorescent perfusion is not seen in the anastomotic area for more than 30 s, a change in digestive tract reconstruction method may be necessary.

The use of a single dimension, fluorescence imaging time, to predict anastomotic perfusion remains controversial. Keouna Pather injected ICG prior to anastomosis in 100 patients undergoing laparoscopic surgery, and visualization of the tube-gastric tip within 60 s was considered adequate perfusion, otherwise the anastomosis was re-established [27]. In contrast, Brian adopted the same 60 s evaluation criteria in a prospective controlled study of 40 cases, but found no difference in anastomotic leak rates between the ICG group and the control group [28]. A prospective study with 84 cases of gastroesophageal anastomosis by Slooter demonstrated [29] that calculation of visualization time from the start of intravenous ICG injection (ICGi). Compared to the group without anastomotic leak, there was no statistically significant difference in the prolonged imaging time of fluorescent agent from injection to the fundus of

the stomach and the anastomosis in cases of anastomotic leaks, but there was a relationship between the prolonged imaging time and anastomotic stenosis. Elke Van Daele reviewed 266 patients with oesophagogastric anastomosis [30] and found that indocyanine green angiography did not reduce the incidence and severity of anastomotic leak (Clavien-Dindo score $\geq$4). Also there was no statistical difference in the incidence of anastomotic leaks in patients with inadequate perfusion compared to those with homogeneous perfusion (30 s as the cutoff value) (19.6 % vs 10.2 %, $p = 0.19$). In conclusion, the criteria for determining the temporal dimension of uneven ICG perfusion varied considerably between studies and may have influenced the findings.

Visual evaluation methods (including calculating the time for fluorescent agent to reach the anastomosis) are relatively simple and easy to implement, with low equipment and system requirements, but these studies have significant limitations: (1) most of them are cohort studies, lacking randomized controlled data. (2) Evaluation criteria are not standardized and are subject to subjective influences. (3) There are variations in the injected dose of fluorescent agents. Therefore, there is a need to integrate objective parameters to quantify vascular perfusion and to develop a corresponding software system to evaluate the anastomosis.

2.2. Quantitative fluorescence-guided surgery (qFI): a promising strategy based on software analysis

2.2.1. Indocyanine green (ICG)

Interpretation in quantitative form is essential to ensure objective and correct fluorescence imaging results. It has been suggested that although repeated injections of ICG may interfere with the visualization, repeated quantitative evaluation of ICG seems to be possible when the software algorithm is slightly modified [45]. Most current studies evaluating perfusion during gastrectomy have been performed on tube stomachs, which facilitates the collection of quantitative data due to the fixed vascular distribution (mainly gastric omental vessels) after tube stomach is made. In general, fluorescence assessment may be affected by patient-related factors (blood pressure, arteriosclerosis of marginal vessels, body mass index) and fluorescence technique factors (dose, time, distance, near-infrared light intensity). In contrast to the heterogeneity that occurs between different observers in qualitative fluorescence evaluations, Nikolaj Nerup invited 10 surgeons to assess anastomotic perfusion in 10 patients with tube stomachs according to the developed quantitative ICG fluorescence software and, subsequently, scored the observed results according to the System Usability Scale (SUS®). In contrast to qualitative fluorescence, quantitative fluorescence reduces overestimation of perfusion and narrows subjective differences between different observers [31]. Table 2 summarizes the studies of qualitative or quantitative fluorescence imaging to evaluate anastomotic perfusion. Most of the current studies were conducted based on ICG, and quantitative methods are more complex to apply in clinical practice. Various visualization software are in the developmental stage, with different developers using different evaluation parameters, and the parameters need to be adapted to particular situations and different surgical platforms.

Quantitative fluorescence imaging was first applied in vivo to assess the effect of different degrees of coronary stenosis on myocardial perfusion. Due to its short half-life, ICG is well suited for repeated measurements, but after several injections, residual ICG stores in the tissue result in persistent fluorescenc that interferes with the field of view. Christian Detter [32] proposed three parameters: background minus peak fluorescence intensity (BSFI), slope of fluorescence intensity (SFI), and time to slope (TTS). BSFI helps to eliminate false high values due to ICG tissue pooling. SFI is independent of background ICG pooling, which is strongly dependent on vascular blood flow and circulatory load, and indicates the elevation of the fluorescence signal over time. TTS can be used as an additional quantification technique, reflecting the lengthening of the pathway from the root of the artery to the distal end of the arcade in response to hemodynamic changes. This therefore somewhat compensates for the disadvantages of repeated ICG injections and reduces misinterpretation of perfusion status caused by visual interpretation.

One of the major advantages of quantitative fluorescence imaging is that objective data, such as blood flow velocities, are used to delineate the "demarcation line" of high-risk areas for anastomotic leaks, as opposed to the "underperfusion" observed with qualitative fluorescence imaging. Nikolaj Nerup demonstrated earlier in animal studies that blood flow in the gastric region correlates strongly with the slope of the fluorescence curve, and that the results measured in different parts of the stomach are independent [33]. Philipp von Kroge [34] selected 20 patients at high risk of anastomotic leak, and found that SFI, BSFI, and TTS were significantly reduced after crossing the demarcation line in the area of insufficient perfusion, and the TTS prolonged with increasing distance between gastric fundus and pylorus. The authors concluded that a decrease of less than 32 % in SFI and less than 23 % in BSFI in the anastomotic region was not associated with anastomotic leakage. In addition to detecting the demarcation line, Nerup et al. also used published algorithms to clinically validate the ability to show optimal anastomotic position after quantitative analysis [35].

Fumitaka Ishige was the first to use a software program (Hamamatsu Photonics K.K, Tokyo, Japan) to quantitatively analyze ICG imaging to assess gastric tube blood perfusion in 2018 [36]. The software allowed the creation of a temporal fluorescence intensity profile to assess blood perfusion over a 5-min period. The value obtained by subtracting the baseline fluorescence intensity from the maximum fluorescence intensity at the surface of the gastric wall was noted as FImax. Tmax was defined as the time between the moment when the intensity started to increase and the moment when it reached its maximum. The software allows surgeons to actively mark regions of interest (ROIs) with a pen or finger on a touch screen during surgery. After intravenous injection of ICG for 30–40s, depending on the selected ROI, a picture of the gastric wall is generated with colour-coded markers, the different colour codes represent changes in the slope of the fluorescence time curve. It objectively showed a decrease in blood perfusion in response to a decrease in FImax and a prolongation of Tmax in the tube stomach making process and at the time of anastomosis, which was not detected by the surgeon's subjective and macroscopic judgment. During gastrectomy, the maximum fluorescence intensity (Fmax) and inflow time point (τ) (the time point at which fluorescence intensity begins to increase at each location) increase at the base of the tube stomach compared with the gastric body due to ligation of the arteriovenous veins and therefore the mean slope (Fslope) decreases. Assuming that the distance from the root of the perigastric artery (the end of the fluorescence signal) to the base of the tube stomach is indicative of anastomotic leakage, there was a significant difference between the base of the tube stomach and the other perfusion

zones in terms of Fmax, Fslope, and τ. Sanne M. Jansen used the cut-off line of Fslope<0.2 [37], and an increase in the distance from the base of the tube and stomach at this cut-off line was associated with anastomotic leak ($p = 0.0005$). In contrast, the distance from the fluorescent demarcation line to the base of the tube stomach seen by the naked eye was not statistically different from the occurrence of anastomotic leak. This study demonstrates the unique advantage of quantitative perfusion-related parameters over naked-eye visualization of demarcation lines.

Many quantitative fluorescence parameters use peak time for dynamic measurements, but in the low perfusion state, peak time occurs late and there is a short observation window period after ICG injection. Haryadi Prasetya proposed a value of relative time-to-threshold (RTT) [38] that can be performed in a short fluorescence imaging acquisition window while constructing a model of a low-flow tube stomach after impaired perfusion. The model suggests that in the low perfusion model, a shorter time to reach threshold predicts worsening of inadequate perfusion. In clinical practice, only a relatively short fluorescence imaging measurement time is required to determine the presence of hypoperfusion, thereby reducing the risks associated with surgery. This study only used hypothetical data and the validity of the model remains to be verified.

In a retrospective analysis of UMIN000030747, Mikito Mori added the parameters of "heterogeneity" and "time" to the assessment of anastomotic leak in gastric cancer [39]. The operator judged the ICG fluorescence images on both sides of the anastomosis at the sixtieth second after injection and divided them into three groups: (1) the homogeneous group (Ho), when the proximal and distal fluorescence intensities across the anastomotic line were equal, (2) the heterogeneous group (He) when the proximal and distal fluorescence intensities across the anastomosis line were unequal, and (3) the faint group (Faint) when the proximal or distal fluorescence images were not visible. There was a statistical difference in the incidence of anastomotic leak in the Ho, He and Faint groups (1.6 %, 2.7 %, and 100 %, $p = 0.001$). Subsequently, the authors defined the time point of intravesical injection of ICG as 0s, the first or second time point of ICG fluorescence appearance on one or the other side of the anastomosis was defined as FT or ST, and the time difference between ST and FT was defined as TD. The study found an increased risk of anastomotic leak with TD $\geq$ 18 s compared to TD $<$ 18 s (50 % versus 1.1 %, $p < 0.001$), similarly, the risk of anastomotic leak for ST $\geq$ 34 s was increased (21.4 % versus 1.2 %, $p = 0.015$). Multifactorial analysis suggested that TD $\geq$ 18 s was an independent risk factor for anastomotic leak (OR = 35.36, $p = 0.027$). The parameters obtained in this study could help in the development of future related software systems.

Quantitative fluorescence optimises the shortcomings of naked eye and empirical evaluation methods and has great research potential. Objective interpretation of quantitative parameters can help surgeons to (1) correctly place anastomoses in well-perfused tissues, (2) decide on the administration of fluids or medications to improve perfusion, (3) improve perfusion by gastric short vein or creation of an extra-arterial vascular anastomosis, (4) re-establishing the anastomosis or changing the reconstruction and (5) select high-risk patients for strict postoperative barium swallow monitoring [40,41]. However, quantitative fluorescence imaging still faces many challenges in gastric cancer surgery. Unlike in wide field of view, quantitative fluorescence imaging systems accurately estimate the optical properties of the fluorescent agent by calibration and thus have made significant advances in neurosurgery and breast surgery, the greater depth of abdominal surgery means that quantitative fluorescence imaging is limited by the depth of tissue penetration. In addition, most studies have focused on the evaluation of perigastric vascular perfusion, while corrective identification of lymph nodes and tumours still faces many difficulties.

In summary the success of visual fluorescence techniques subsequently led to the development of quantitative fluorescence techniques, as the latter highlighted the inherent limitations of visual assessment (subjectivity, inter-observer dependence, inaccurate measurements, reduced sensitivity to residual disease). The future development of fluorescence-guided surgery will require the collaborative research of multiple fields such as optical equipment, probe technology, and software development.

2.2.2. Other methods for quantitative assessment of optical imaging

In addition to the fluorescent agent injection method, other quantitative assessment methods of optical imaging have been proposed, among which laser Doppler flowmetry (LDF) [25], laser scatter contrast imaging (LSCI) and thermography (TI), and Hyperspectral Imaging (HSI) provide information on perfusion and changes in blood flow during anastomotic creation. These methods do not require injection of fluorescent agent, avoiding the problem of fluorophore retention in the tissue due to repeated perfusion during evaluation. Table 3 summarizes potential optical imaging techniques that provide quantitative data directly, but the numerical reliability and clinical applicability need to be revised and validated in larger clinical studies.

2.2.2.1. Laser Scattered spot lining imaging (LSCI). Laser Scatter Lining Imaging (LSCI) displays colour thermograms of real-time tissue blood volume by capturing coherent laser interference with red blood cells [104]. LSCI is suitable for real-time and non-contact assessment of microcirculation and uses a low-power laser light source to illuminate the tissue of interest. The resulting interference is imaged on a camera in what is known as a scatter pattern, and is capable of varying in response to red blood cell movement at a rate corresponding to the blood flow. This blurring or loss of contrast is quantified as laser scatter perfusion units (LSPU), with higher LSPU values corresponding to better tissue perfusion. Unlike ICG, LSCI perfusion detection is real-time (latency <150 ms) and does not require fluorophore injection [43]. It is well known that 2–4 min after ICG injection is the optimal observation time window, and LSCI and ICG modalities show similar temporal and spatial precision at less than 2 min, whereas the temporal and spatial precision of LSCI is significantly better than that of ICG at observation times >5 min [44].

It is worth noting that LSCI has a narrower application and is only used to assess ischaemia because 95 % of the signal detected by LSCI comes from the top 700 μm layer of the tissue (serosal layer), whereas ICG has been shown to penetrate from a few millimetres to a centimetre (including the mucosa). Jonas Hedelund Rønn's experiments on 19 animals have demonstrated that ICG might be more sensitive than LSCI for assessing anastomotic perfusion, as mucosal ischaemia may occur prior to full gastric wall ischaemia. Unlike

ICG, LSCI allows continuous assessment of perfusion before, during, and after anastomosis establishment. As grading ischaemic changes in the whole gastric wall is challenging, combined LSCI and ICG may be useful in such cases.

LSCI is limited by distance and angle, and it is challenging to ensure that the target structures are located at the appropriate distance and angle of the camera, making it difficult to apply in minimally invasive procedures. Notably, however, an ActivSight™ imaging module (Activ Surgical, Boston, MA) integrating ICG fluorescence imaging and LSCI technology was recently reported for the first time by Yao Z and initially applied to 67 robotic or laparoscopic cholecystectomy, colorectal and bariatric surgeries [46]. The results of this prospective, multicentre study demonstrated that LSCI could assess intestinal perfusion at a similarly high rate (97.5–100 %) compared to ICG visualization. Recently, Aurelia Wildeboer reported laparoscopic LSCI in a porcine model to assess local intestinal perfusion during the construction of intestinal anastomoses. The authors designed PerfusiX-Imaging, a laparoscopic perfusion imager, as an add-on to the laparoscopic system [105]. The LSCI was able to provide real-time, continuous anastomotic perfusion information on its own, shows the potential of laparoscopic LSCI.

2.2.2.2. Thermal imaging (TI). Thermal imaging has been used for screening, diagnosis and treatment of neurological and cardiac disorders, and the gastric surface temperature measured by TI may be influenced by room or body temperature, and a simple conversion of temperature to tissue perfusion is questionable. To allay this concern, Katsunori Nishikawa attempted a quantitative assessment using the Anastomotic Survival Index Threshold score (AVI score), based on TI data from more than 250 patients. The AVI score was calculated by multiplying the perigastric artery length ratio (L-GEA) with temperature retention in graft perfusion (TRr), AVI score $\leq$0.61 (2 % vs. 28 %, $P < 0.001$) suggests an increased risk of anastomotic leak [143]. TI has advantages for blood flow distribution and its quantification and is reproducible, but compared to ICG, TI can only observe static photographs and does not clearly show vascular structures. The use of TI in gastrointestinal surgery is still limited to experimental models of intestinal ischaemia, but preliminary studies have been conducted in laparoscopic and open colorectal surgery.

2.2.2.3. Hyperspectral Imaging (HSI). Hyperspectral imaging can simultaneously acquire two-dimensional spatial information and one-dimensional spectral information of biological tissues, providing finer spectral features for biological histological studies. HSI measured by endoscopic/minimally invasive systems has been used in the clinic [47], and HSI is suitable for checking the perfusion of the remnant stomach during open surgery. Barberio et al. translated the HSI technique into virtual reality (HYPER) in animal experiments, overcoming the limitation that the information is given on a screen without corresponding spatial data [48]. However, assessment of perfusion in confined spaces and after digestive tract reconstruction is two problems for HSI system. Sebastian Hennig used both imaging techniques for the first time in the evaluation of 13 gastro-oesophagectomy and reconstruction surgeries. HSI and ICG are able to complement each other's strengths in the quantification of tissue perfusion by means of their respective software systems (The TIVITA® Suite software; Image J, Vision Sense 1.52, etc.), which will broaden the scope of image-guided surgery [49]. HSI is easy to perform and observations are reproducible, but difficult to assess after digestive tract reconstruction. Simultaneous intraoperative HIS and ICG imaging, both of which are feasible but needs to be validated in large prospective trials.

2.2.2.4. Laser Doppler Flowmetry (LDF) and visible light spectroscopy (VLS). Laser Doppler Flowmetry (LDF) uses a laser to measure the velocity of red blood cells (rHb) by Doppler shift. Visible light spectroscopy (VLS) enables significant differences in the absorption spectra of oxyhaemoglobin and deoxyhaemoglobin. An increase in oxyhaemoglobin content in the mucosa indicates adequate perfusion and conversely a decrease in oxyhaemoglobin content suggests inadequate perfusion. Intraoperatively, the values and waveforms of haemoglobin saturation (StO_2), relative haemoglobin, flow and velocity can be observed in real time on monitor [50]. Nathkai Safi performed thoracoscopic gastro-oesophagectomy in 10 patients with oesophageal cancer after neoadjuvant therapy [51], and intraoperatively, the gastric wall perfusion was detected simultaneously by laparoscopy with a 2.6 mm microcatheter. This study found that after anastomosis the mean decrease in StO_2 of 49 % (25%–69 %) in the three patients who developed anastomotic leaks, compared with 39 % (32%–46 %) in those who did not have anastomotic leaks. After anastomosis, rHb increased from baseline to 61 % (33%–147 %), and 17 % (0–38 %), respectively in the patients with and without leaks. In addition, patients with and without leak had similar changes in mean flow rate after anastomosis (11 % vs 12 %)., and there was no statistically significant difference in the increase in mean tissue blood flow (36 % vs 26 %). Intraoperative real-time detection of tissue perfusion by LDF combined with VLS is feasible, and this method has also been validated in ischaemic bowel disease, among others. Patients with anastomotic leaks have more severe local tissue perfusion deficits (reduced StO_2) and venous congestion (increased rHb). The use of LDH combined with VLS is relatively easy to detect, but assessing residual gastric perfusion with different gastric resection modalities requires different quantitative values, and therefore more research is needed to optimise clinical application.

In conclusion, LDF, VLS, LSCI, TI and HSI methods for detecting gastric perfusion are capable of obtaining quantitative parameters with high reproducibility. However, they all suffer, to varying degrees, from disadvantages of, cumbersome operation, unavailability of imaging equipment, space constraints and inability to observe tissue structure. The visual images of real-time perfusion by ICG makes the results easy to be interpreted, but lacks uniform quantitative parameters to improve the accuracy. Based on existing studies, LSCI combined with ICG holds the most promise for accomplishing clinical translation of laparoscopic surgery. In addition to this, the emergence of digital image analysis software programs featuring automated analysis based on Artificial Intelligence represents a rapidly growing field. Convolutional neural networks (CNNs) are one of the most commonly used artificial neural networks today. There are studies that add this proprietary deep learning algorithm to established laser scatter contrast imaging (LSCI) [52]. In conclusion, current imaging techniques seem to struggle with reproducibility, simplicity, and accuracy, and the development of software programs is highly anticipated in the field of perfusion imaging.

3. Vascular navigation and margin determination

3.1. Vascular navigation

Fluorescence imaging offers some advantages, but real-time rendering of 3D CT images remains the most accurate method. In laparoscopic or robotic radical gastrectomy, vascular injury may occur due to variations in vessel alignment or errors in visual discrimination, which may lead to splenic infarction, stump or anastomotic leak, and hepatic impairment. Meanwhile, some function-preserving surgeries, such as Laparoscopic pylorus preserving gastrectomy (LPPG), require a high level of operator, and may result in impaired gastric emptying and difficulties in lymph node dissection.

Real-time rendered 3D CT image navigation technology enables real-time, clear intraoperative 3D modelling of perigastric vessels. The surgical navigation system supports intraoperative understanding of the anatomical information, and patient-image alignment is accomplished by aligning preoperative CT spatial images with the patient's coordinate system, showing the anatomical structures at key locations and guiding the optimal location for vessel resection or preservation. There has been previous study using customised software programs designed specifically for laparoscopic gastrectomy to provide 3D vascular images [53], but achieving accurate alignment in laparoscopic surgical navigation is very challenging due to soft tissue deformation and intraoperative displacement. Recently, it has been reported to improve the imaging accuracy by incremental matching [54]. The authors anchored "landmarks" at the root of the vessel, which moved little during operation and identified them by the software, which guides the subsequent stages of the surgery.

ICG imaging is fast and easy to perform, and is used to identify intraoperative variant vessels, reducing the difficulty of vascular dissection, especially in operations involving functional and organ preservation, such as subpyloric artery dissection, splenic hilar lymph node dissection, and identification of variant left hepatic artery. Several studies have shown a surprising detection rate of variant vessels after the use of ICG, which cannot be detected by empirical judgment. Kim et al. used ICG to identify the type of subpyloric artery anatomy in 20 robotic and laparoscopic surgeries [55,56], 20 % (4/20) of patients identified subpyloric arterial anatomy that was distinct from empirical judgement. Ishikawa et al. with the aid of intravenous ICG in robotic distal gastrectomy, the presence of the splenic collateral artery was identified in 6 of 12 patients [57]. Similarly, Joong Ho Lee reviewed 31 patients undergoing minimally invasive radical gastrectomy with an anomalous left hepatic artery, only 6 (19 %) patients had an anomalous left hepatic artery reported on preoperative CT, and the rest were identified by ICG [58]. In addition, there are some case reports that ICG real-time imaging is used in special types of gastrectomy with high requirements for vessel preservation, such as (1) vascular status of the remnant stomach was assessed by ICG in patients with a history of distal gastrectomy undergoing pancreatectomy, (2) distal gastrectomy after coronary artery bypass grafting, preserving the right vessels of the gastric omentum through ICG imaging to avoid insufficient coronary blood supply, or (3) laparoscopic distal gastrectomy (LDG) combined with spleen-preserving distal pancreatectomy (LSPDP) requires protection of the gastrosplenic ligament and preservation of the blood supply to the remnant stomach [59–61].

In some special operations, ICG provides real-time imaging of the local vascular anatomy, which helps to reduce the difficulty of the procedure, reduce splenic infarction, and protect the blood supply of the residual stomach. ICG is limited by the thickness of the covered tissue which affects its accuracy. Real-time rendering of 3D CT images is still considered to be the most accurate method for perigastric vascular navigation. However, ICG is easy to operate intraoperatively, hardly occupies the operation time, and can even optimise the operation process in some special cases, while real-time 3D CT image navigation is still complicated and unable to evaluate the tissue perfusion in real time, so its application in the clinic has not yet been popular.

3.2. Cutting edge determination

In minimally invasive surgery, the lack of palpation makes it difficult to locate tumours during surgery, especially in oesophagogastric tumours. Takeshi Omori observed 107 cases of proximal or gastro-oesophageal tumours [123], where ICG was injected into the margins of the tumour one day prior to surgery via endoscopy. Intraoperative ICG labeling was detected in all cases, and tumour infiltration in the oesophageal and gastric resection lines based on ICG fluorescence images was negative. In patients with carcinoma of the gastroesophageal junction, the mean proximal apparent borders were 27 mm (2–60 mm) and the mean distal apparent borders were 50 mm (5–40 mm), and in patients with distal gastric cancer, the mean proximal and distal apparent borders were 34 mm (5–65 mm) and 45 mm (7–180 mm), respectively. No anastomosis-related complications or pancreatic leak occurred in postoperative period, and only one patient (0.9 %) had a combined Clavien-Dindo grade III pleural effusion. Submucosal ICG injection during gastrectomy ensures a resection margin of 28 mm or greater and avoids intraoperative endoscopy. However, there is still no substitute for intraoperative frozen pathology to determine negative resection margins for gastroesophageal junction cancer.

In contrast, the lack of changes in the serosal layer of early gastric cancer, especially in minimally invasive procedures, makes it challenging to determine the line of surgical resection based on tumour location. Therefore, preoperative endoscopic clip localisation remains recommended for early stage cancers [62].

4. Assessment of lymph node drainage

The anatomical variations in gastric lymphatic drainage make lymph nodes within adipose tissue difficult to identify with the naked eye, and reducing the accurate perception of D2 lymph node (LN) clearance intraoperatively leads to a higher likelihood of incomplete eradication. In 2015, the Dutch Gastric Cancer Trial reported a high incidence of undergoing low-quality D2 lymph node dissection

(84 %), acknowledging the complexity of this procedure [63]. Lymph nodes in close proximity to large vessels undergoing dissection are challenging and often lead to unexpected intraoperative injuries, and inadequate lymph node dissection and the omission of lymph nodes beyond the D2 group are known to result in high postoperative recurrence and mortality rates [64,65]. Therefore, the application of intraoperative navigation techniques to assist systematic and complete lymph node dissection is crucial for radical gastrectomy. Currently, navigational surgery of lymph nodes is mainly by virtue of each fluorescent agent, and purely optical imaging techniques have not been reported in studies. In recent years, ICG fluorescence imaging to guide radical gastrectomy has attracted much attention in the field of gastrointestinal surgery. For example, ICG imaging helps to distinguish lymph nodes and blood vessels, shorten the operation time in the subpyloric and splenic regions, shorten the exposure time of perigastric vessels, reduce intraoperative injury, and help function preservation [66]. However, the application of ICG imaging systems in clinical practice is still in its infancy, and there are still some problems to be solved as follows.

4.1. Selection of fluorescent dye injection route

There is no consensus on the imaging effect of fluorescent dyes, either by transmucosal or subserosal injection, which are mostly selected based on surgical approach [67]. In open surgery, ICG is usually injected intraoperatively through the serosa of gastric wall, and the average imaging time of lymph nodes after ICG injection is 178.8 ± 86.1 s. Therefore, 1 ml (0.1 mg) injected into the periphery of the lymph nodes 15 min before lymph node dissection at serosal layer, but the observable time of the serosa side of the injection only lasts for a few hours. After submucosal injection of ICG, the lymph nodes are visualized later and thus are mostly used for minimally invasive surgery completed endoscopically 12–24h before surgery. Submucosal injections are more difficult and require a learning curve, as deep injections cause intravascular injections that result in complete blurring of neighboring organs. In the case of extra-luminal leakage, even small amounts of ICG can contaminate the surgical field [68]. To minimize ICG leakage, the "tattoo" method (0.5 ml of saline followed by 0.5 ml of low-concentration ICG) or the "sandwich" method (saline-ICG-saline) have been used [69]. Park et al. [70] suggested that serial subserosal injection of ICG along the greater and lesser curvatures of the stomach were more appropriate than peritumoral submucosal injections, because it was necessary not only to identify the lymph nodes, but also to show the network between all the perigastric lymphoid tissues, but the number of visualized lymph nodes obtained by this method was relatively low, and it was difficult to use in minimally invasive surgery. It should be noted that the concentration of ICG solution should not be too high, otherwise the excessive fluorescence intensity will hinder the observation of the tissues, and a low concentration (0.05 mg/ml) is recommended.

4.2. Difficulty in recognition after neoadjuvant therapy

Although neoadjuvant therapy and lymph node metastasis appeared to limit the effectiveness of ICG imaging, intraoperative ICG-guided lymph node dissection was the only independent factor influencing the acquisition of a median total lymph node count. Huang's study confirmed [71] that the ICG technique maintained significantly more lymph node harvest in patients who achieved stable or progressive disease after neoadjuvant chemotherapy. But on the contrary, another retrospective study of 102 cases from Francesco [72] found that although the median number of lymph nodes obtained was significantly higher after intraoperative ICG guidance (44 vs 32, $p = 0.004$), this difference was not statistically valuable in neoadjuvant patients ($p = 0.312$). These results could support the hypothesis that tumour and positive lymph node shrinkage after chemotherapy leads to reduced effectiveness of ICG. It is well known that partial and complete remissions to neoadjuvant therapy result in varying degrees of tumour regression, and the degree of tumour regression can often be measured by the amount of fibrosis that replaces the cancerous tissue, thus leading to difficulties in identifying lymph node tissue by ICG.

4.3. Limitations of metastatic lymph node imaging

Most studies seem to suggest that lymph node dissection by ICG visualization is of no benefit in advanced gastric cancer. A retrospective study of 56 cases [73] showed that the perioperative safety of the ICG group was comparable to that of the control group, and there was a significant advantage in the number of small lymph nodes (<5 mm) cleared in the ICG group in terms of the effect of lymphatic dissection (21.84 vs 16.24, $p < 0.001$), while there was a significant advantage in the number of perigastric lymphatic (groups 1–7) dissections (22.89 vs 20.29, $p = 0.007$), and the improvement in the number of extragastric regional lymph nodes (groups 8–12) cleared (11.72 vs 9.61, $p = 0.022$) had little advantage over empirical clearance. This may be due to the fact that small lymph nodes <5 mm are more likely to be hidden in adipose tissue and difficult to identify by conventional laparoscopy. However, the authors also found some empirically suspicious positive enlarged lymph nodes that were not visualized after intraoperative ICG injection.

A 266-sample, single-center, prospective, randomized, controlled study evaluating the lymph node detection rate of ICG lymph node navigation surgery in cT1-cT4a radical gastrectomy demonstrated more comprehensive data. The study found that metastatic lymph nodes did not achieve a satisfactory benefit [74]. The authors found that the mean number of lymph nodes retrieved in the ICG group was significantly more than that in the non-ICG group (50.5 vs 42.0, $p < 0.001$), with no difference in complication rates. In distal gastrectomy (DG), the number of lymph nodes obtained within the lymph nodes at stations 4, 6, and 7 was higher in the ICG group than in the non-ICG group. In total gastrectomy (TG), the number of lymph nodes within stations 4sa, 7, 11d, and 12a was higher in the ICG group than in the non-ICG group. Not only that, in the ICG group, a mean of 27.3 fluorescent lymph nodes and 23.2 non-fluorescent lymph nodes were detected, more lymph nodes were obtained in the fluorescent lymph node stations than in the non-fluorescent lymph node stations (DG: 5.27 vs 2.15, TG: 4.89 vs 2.04). In addition the ICG group had a higher number of perigastric

and extragastric lymph node acquisitions than the empirical group, and the mean total number of lymph nodes retrieved in the D2 range was higher than that of the non-ICG group (49.6 vs 41.7, $p < 0.001$). However, this study found that the number of metastatic lymph nodes at all sites was not significantly higher in the ICG group than in the non-ICG group, and the diagnostic sensitivity and specificity of fluorescence imaging for metastatic lymph nodes were only 56.3 % and 46.1 %, respectively.

The limitation of metastatic lymph node imaging may be because ICG is injected around the tumour. Although fluorescence can show lymphatic drainage from the tumour, non-fluorescent station lymph nodes may not be fluorescently visualized because the cancer cells do not drain through the lymphatics of the primary tumour, resulting in missed lymph node clearance at non-fluorescent stations. In advanced gastric cancer, patients with jump metastases or due to obstruction from the primary tumour to the lymphatics may have false-negative ICG results. Watanabe's lymph node visualization study indirectly demonstrated the limited benefit of ICG staining for gastric cancers requiring D2 or even extended lymph node dissection, with metastatic lymph nodes distributed beyond D1+ in 54 % of patients with progression, and D2 metastatic lymph nodes (e.g.,No.12a) not being illuminated by ICG in some patients [75]. For further investigation, Ji-Hyeon Park used ICG fluorescence imaging and different colours of tissue-marking pigment (TMD) to mark different lymph node regions [70], and constructed a perigastric lymphatic network map by combining the pathological findings of each lymphatic site to show a more complete topographical map of ICG-stained and unstained lymph nodes including metastatic information. The subjects of the study were all progressive gastric cancers, and the number of lymph nodes was compared with the number of lymphatic stations instead of lymph nodes. Metastatic lymph nodes were seen in 8 patients (28 stations in total), and ICG staining was seen in only 40 % (11.1%–75 % per case) of the metastatic lymph nodes within the lymph stations. Of the lymphoid stations with metastases, 21 (75.0 %) lymph node regions were covered by ICG, whereas metastatic lymph nodes actually stained by ICG were present in only 16 lymphoid stations (57.1 %). Therefore ICG imaging is not recommended for selective lymph node dissection in patients with progressive disease.

A recent prospective randomized controlled study of 195 cases similarly demonstrated that ICG fluorescence surgery was not beneficial for D2 lymph node dissection [76]. The number of total lymph nodes harvested in the ICG group (49.55 vs 44.44) as well as the number of lymph nodes in the D1+ group (28.54 vs 24.13) was significantly higher than that of the control group, but the difference in the number of lymph nodes at the D2 station was not statistically significant (21.05 vs 20.38). Similarly, although the ICG group harvested more number of metastatic lymph nodes in total metastatic lymph nodes (6.45 vs 3.33) and metastatic D1 station (5.06 vs 2.40), there was no difference in the number of metastatic lymph nodes in D2 group (1.39 vs 0.92). Notably, the total operative time (198.22 vs 202.50 min) as well as the reduction in lymph node dissection time (90.90 vs 93.74 min) and the reduction in bleeding (27.51 vs 32.02 ml) in the ICG group did not have a significant advantage over the control group. In addition, no survival benefit was found: 2-year overall survival was 87.8 % in the ICG group versus 82.9 % in the control group ($p = 0.304$), 2-year DFS was 86.0 % in the ICG group versus 80.7 % in the control group ($p = 0.471$).

In another retrospective study of 168 laparoscopic and robotic surgeries [77], the fluorescent lymph node dissection (FL) group had a higher overall survival (FL group: 96.9 % vs non-FL group: 88.9 %, $p = 0.334$) and recurrence-free survival (FL group: 90.5 % vs non-FL group: 65.5 %, $p = 0.054$), although there was no statistical difference. However, in patients without lymph node metastasis, the recurrence-free survival rate was significantly higher in the FL group than in the non-FL group (100 % vs 67.1 %, $p = 0.017$). Of note, in this study, 54 % of the patients in the FL group had fluorescence at the splenic hilum, implying that not all patients had lymphatic connections between the tumour and lymph nodes. Similarly, this study noted that the specificity (40.5 %) and positive predictive value (12.3 %) of fluorescent lymphography were low because ICG is not a cancer-specific tracer. Even without an increase in the number of positive lymph nodes, there are no reliable studies demonstrating the long-term survival benefit of lymph node navigation surgery for progressive gastric cancer, but some studies have suggested that an increase in the number of lymph node dissection procedures in patients with lymph node-negative gastric cancer may provide a survival benefit by reducing the potential for micrometastasis and lymphatic invasion [78,79].

There are also arguments to explain the above phenomenon, suggesting that the non-integral resection of lymph nodes may be one of the potential reasons for the lack of survival benefit in the ICG group. Previous studies have reported that lymph node noncompliance has a significant impact on the long-term survival of gastric cancer patients [80]. Lymph node noncompliance was defined as more than 2 expected lymph node stations that were not removed during surgery. Whereas surgeons can use ICG imaging to assess the completeness of lymph node dissection and effectively reduce lymph node noncompliance by dissecting the residual lymph nodes. Chen's study found that the lymph node noncompliance rate was lower in the ICG group (31.8 %) than in the non-ICG group (57.4 %) [81], with a statistically significant difference in lymph node noncompliance in the total gastrectomy group ($p = 0.002$), and in the Distal gastrectomy ICG group was lower than the non-ICG group but not statistically different ($p = 0.13$), which may be attributed to the relative ease of distal gastrectomy to achieve complete lymph node dissection. However, there is no subsequent survival follow-up data from the study on the reduction of lymph node noncompliance by ICG.

4.4. Sentinel lymph node dissection and early gastric cancer

Unlike progressive gastric cancer, ICG-guided surgery for early gastric cancer focuses more on reducing the clearance area and preserving function.

The incidence of lymph node metastasis in patients with early gastric cancer (EGC) ranges from 8.0 to 20.0 % [82]. The remaining patients without lymph node metastasis may not benefit from extensive lymph node dissection. Over the past decade, surgical or endoscopic techniques for sentinel lymph node (SLN) detection and resection have been progressively developed through iterative trials, and researchers seem to have reached a consensus [83]. Sentinel lymph node navigation (SLN) surgery has been investigated for gastric cancer to limit and adjust the extent of lymph node dissection, reduce surgical complications and improve quality of life. The

presence of lymph node metastases determines not only the extent of lymph node dissection, but also the extent of resection of the primary tumour during gastric cancer surgery. Standard perigastric lymph node dissection compromises the blood supply and innervation of the stomach itself; therefore, extended gastrectomy should be accompanied by standard lymph node dissection even if the primary tumour is very small. Unlike breast cancer surgery, secondary surgery for gastric cancer is technically demanding. Prior function-preserving gastrectomy interferes with the establishment of a new reconstruction, which may increase the risk of post-operative complications (e.g., leakage). In addition, gastric cancer may have more than 10 antecedent lymph nodes [84], therefore fluorescence imaging is valuable for sentinel lymph node clearance in early gastric cancer. However, the optimal technical approach for intraoperative assessment of the sentinel lymph nodes remains to be determined.

Unlike advanced gastric cancer, ICG has higher sensitivity and specificity for metastatic lymph nodes in studies targeting early gastric cancer. Chang Min Lee collected 815 lymph nodes from 20 patients with stage I gastric cancer, and the mean number of lymph nodes removed per patient was 40.8, with sensitivity, specificity and false-negativity of 100.0 %, 94.4 % and 0.0 %, respectively [85]. A prospective single-center study of early gastric cancer by Gyu Kwon [86] demonstrated that the mean total number of lymph nodes obtained in the ICG group was greater than that in the empirical group (48.9 vs 35.2, $p < 0.001$), and the number of lymph nodes obtained in the ICG group was significantly higher than the control group, both in perigastric lymph nodes (stations 1,2,3,4,5 and 6) and in the extragastric (stations 7,8,9,11 and 12a) region were significantly higher in the ICG group than in the control group (28.8 vs 23.5, $p = 0.02$, 19.9 vs 11.3, $p < 0.001$ respectively). The number of fluorescent lymph nodes obtained was 23.9 (48.9 %) out of a mean of 48.9 lymph nodes, which was not different from that of advanced gastric cancer.

The standard for additional surgery after ESD is radical gastrectomy plus systemic D1 + lymph node dissection, and most patients do not require systemic lymph node dissection after ESD. As an alternative, sentinel lymph node navigation surgery (SLNNS) can be used to minimize the extent of post-ESD lymph node dissection. It has been suggested that the lymphatic network in the submucosa is disturbed after ESD due to scar formation and fibrosis in the submucosa. This may prevent visualization of lymphangiography, and there are also concerns about the rate of SLNNS false negatives and the presence of jump metastases. A retrospective study by C. K. Roh of 290 patients who underwent robotic D1+ surgery after ESD suggests [87] that an average of 31.5 fluorescent lymph nodes were obtained per patient in the ICG group, and 16.2 non-fluorescent lymph nodes. The number of lymph node stations was less in the fluorescent group than in the empirical group (9.4 vs 9.6, $p = 0.031$), but the overall number of lymph nodes obtained was increased (47.7 vs 40.7, $p = 0.001$). The number of perigastric lymph nodes was increased in the fluorescent group (31.5 vs 25.9, $p = 0.001$), but there was no difference in the number of extragastric lymph nodes (16.2 vs 14.8, $p = 0.137$). The sensitivity of identifying positive lymph node metastasis based on fluorescent lymph nodes was 88.9 %, the specificity was 34.0 %, and the positive predictive value (PPV) and negative predictive value (NPV) were 0.3 % and 99.9 %, respectively. In contrast, based on the fluorescent lymph node site, the sensitivity for detecting lymph node metastasis was 100 %, specificity was 23.0 %, PPV was 1.3 %, and NPV was 100 %. Therefore, postoperative fluorescent lymph node visualization of sentinel lymph node clearance after ESD remains feasible. The study did not follow up survival, and the long-term effects of the strategy of omitting the non-fluorescent station during clearance are unclear.

In addition to fluorescence imaging, the accuracy of sentinel lymph node detection depends on the method of pathological examination as well as the lymph node sampling method. The Japanese Clinical Oncology Group (JCOG) Gastric Cancer Surgery Study Group published a multicentre prospective study [89], where a high false-negative rate and the necessity of a learning curve, together with the pathological examination of only a single frozen section, were the limitations in detecting metastases in the antecedent lymph nodes.

Indeed, due to the discrepancy between the interpretation of frozen sections and the final results of permanent sections, and since the extent of surgery critically depends on the intraoperative pathological findings during the navigation procedure of the anterior sentinel lymph nodes in gastric cancer, a consensus is needed on pathological assessment and its standardisation in order to correctly diagnose lymph node metastases during surgery [90]. Intraoperative assessment by frozen section analysis has been adopted as a standard procedure in many specialized centres to perform simultaneous sentinel lymph node dissection and avoid secondary surgery. However, some surgeons remain reluctant to adopt these intraoperative procedures, reasons for this include the fact that intraoperative assessment increases the duration of the procedure and that there is a discrepancy between intraoperative pathology and permanent histological reports, which may have a certain false-negative rate (11.1%–53.8 %) [91,92]. Although some enhanced intraoperative techniques (e.g., multistep sectioning, rapid IHC, RT-PCR, or OSNA) have been reported to improve the ability to identify a positive SLN, these enhancements may lead to false positives, prompting unnecessary surgical scope. Not only that, but the inclusion of enhanced methods of examination during intraoperative testing is quite labour intensive and time consuming, and a significant amount of lymph node tissue is lost in the process, which will prevent accurate diagnosis by final standard histopathological examination and increase the risk of metastasis due to lymph node leakage.

The concept of gastric lymphatic basin clearance was first proposed by Miwa et al. [93] to minimize the likelihood of missed metastases, especially during laparoscopic surgery. The gastric lymphatic basin is considered to be orientated along five major arteries: the left gastric artery region, the right gastric omental artery region, the left gastric omental artery region, the right gastric omental artery region, and the posterior gastric artery region. Jump metastases are present in 3.4 % of patients with cT1-2N0 gastric carcinoma, but the majority of these metastases are confined to the sentinel lymph node basin, and even by the most sensitive RT-PCR analyses, only 0.7 % of patients have metastases outside the sentinel basin metastases. Kitagawa suggested that the clinical application of intraoperative sentinel lymph node sampling should consider sentinel lymphatic basin dissection [94,95], which could reduce false negatives in SLN due to sampling errors or jump metastases. The Japanese Society of Sentinel Node Navigation conducted a large prospective multicentre study [96], which included 397 patients with early gastric cancer. The detection rate of 97.5 % (387/397), sensitivity of 93 % (53/57) and accuracy of 99 % (383/387) were compared for SLN examination. Surprisingly, the false-negative rate was only 1 % (4 cases). Three of these four patients had pathological lymph node metastases only in the lymphatic basin (including the

SLB and downstream lymphatic regions). The other patient had metastases outside the lymphatic basin and the primary tumour was more than 4 cm. These results suggest that early gastric cancer (EGC) is mainly operated in the "lymphatic basin" rather than in the "sentinel lymph nodes".

4.5. Other lymph node imaging methods

As with limitations in other applications, fluorescent lymphography has low specificity in detecting LN metastasis. Since ICG is not a tumour-specific fluorescent agent, thus the extent of fluorescent lymphography-guided lymph node dissection is increased [88].

4.5.1. Three-dimensional imaging simulation technique

Fluorescent tracer technology can help to localize gastric cancer-related lymph nodes during surgery, but this technology cannot show the spatial positional relationship between lymph nodes to be cleared and blood vessels and organs. In recent years, three-dimensional (3D) simulation technology has been applied to liver, vascular, maxillofacial and other surgical procedures, but less research has been done on its application in gastrointestinal surgery. It can replace the enhanced CT image of a specified site with an accurate and clear 3D image, mark and extract the 2D information of organs (liver, pancreas, spleen, stomach), tumours, arterial and venous blood vessels, and lymph nodes through a fast segregation algorithm, and generate 3D real-time images by the system. Accurate organ volume and stereotactic information is provided for preoperative planning and intraoperative navigation. One of the major challenges of 3D reconstruction is the difficulty of fully matching real-time images of tissues to preoperative CT due to intraoperative pulling and shifting. This challenge is expected to be solved in the future.

The anatomy of the superior margin of the pancreas is complex, and interactive computer-assisted system (CAS) 3D reconstruction can help to minimize the difficulty of lymph node dissection at the superior margin of the pancreas. Liu et al. [97] used laparoscopically-assisted distal gastrectomy in 56 cases. The 3D reconstruction group was superior to the control group in terms of suprapancreatic lymph node dissection time, number of unnecessary intraoperative injuries, and number of suprapancreatic lymph node dissection (29.00 vs 37.07 min, 2.53 vs 3.57 times, and 13.64 vs 10.75 times, respectively), and the difference was statistically significant ($p < 0.05$). However there was no significant advantage of 3D reconstruction in terms of the number of lymph nodes cleared, except in the region of the superior margin of the pancreas.

4.5.2. Carbon nanoparticles

Carbon nanoparticles have lymphatic tropism, after injection the particles can follow the lymphatic vessels around the tumour and accumulate in the lymph nodes making them dark and detectable by the naked eye. Wang reviewed 50 cases of progressive open D2 radical surgery and there was no significant difference in harvested lymph nodes between subserosal injection of carbon nanoparticles compared to the controls (45.7 vs 39.2). Carbon nanoparticles were less selective for metastatic lymph nodes, with accuracy, sensitivity, specificity, and false negative rates of 57 %, 28 %, 62 %, and 72 %, respectively [98], in addition to inadvertent leakage of nanocarbon that would severely contaminate the surgical field under the naked eye.

4.5.3. The "dual tracer" technique

Multiple tracers are used in conjunction with ICG, known as the "dual tracer-guided technique", to compensate for the lack of specificity of ICG in targeting lymph nodes. Tracers that may have potential include 5-aminolevulinic acid (5-ALA), sodium fluorescein (SF), and nanocolloids (Nanocoll), which specifically accumulate in cancer cells and provide fluorescent signals that do not overlap in excitation and wavelength with ICG [99]. The fact that the molecular sizes and excitation and emission wavelengths of bimolecular tracers do not overlap with each other is the basis for the ability of bimolecular tracers to complement each other's strengths. Osterkamp explored the feasibility of simultaneous injections of ICG and sodium fluorescein (SF) in 10 animal models [100]. Due to the differences in molecular sizes, protein-binding capacity, and lipid solubility ICG distribution is mainly confined to the intra-lymphatic space, whereas SF is more likely to diffuse into the surrounding tissues. Conversely, adsorption of ICG onto nanocolloids increases its hydrodynamic diameter, which may be better retained in the sentinel lymph node, thereby reducing staining of the second layer of lymph nodes and allowing intraoperative identification of true sentinel lymph nodes. Tummers [120] showed that ICG-Nanocoll dual tracing had an overall accuracy of 90 %, with an increased T-stage associated with lower accuracy, and accuracy rates for pTx, pT1, pT2, pT3, and pT4 were 100 %, 100 %, 100 %, 90 %, and 0 %, respectively. The ability of dual tracing to detect fewer sentinel lymph nodes and the ability to detect positive lymph nodes outside the anatomic plane greatly improves the clinical applicability of using NIR fluorescence imaging for sentinel lymph node detection in gastric cancer.

4.5.4. Radioactive colloids

An important advantage of radioactive dyes is the objective measurement of radiation intensity, the long residence time in the lymph nodes, the ability to detect sentinel lymph nodes even in thicker adipose tissue, and the excellent identification of obese patients [101]. The dual tracer method utilizing radioactive colloids (technetium Tc 99m tin colloid, 99mc sulfur colloid, and 99mc antimony sulfur colloid) and dyes (isothiocyanine blue, indocyanine green) was earlier considered to be a reliable method for stable detection of SLNs in patients with early gastric cancer, both are injected transmucosally under preoperative endoscopy. After introduction of a special gamma detector at the needle end of the trocar for laparoscopic surgery, the dye allows real-time observation of lymphatic flow. A multicenter prospective study demonstrated that for early gastric cancer, the detection rate of sentinel lymph nodes by radiocolloid was 98 %, with a positive predictive accuracy of 99 % [94]. However, radioisotope tracers are expensive, require additional gamma probes, and require a radioactivity control area when using radioisotopes, with many limitations on use and safety [102].

A SWOT analysis of lymph node navigation surgery in gastric cancer is described in Table 4. As mentioned earlier, the lymph node fluorescence navigation technique for gastric cancer does not seem to be beneficial for progressive gastric cancer, but there is value in applying it for selective lymph node dissection and function preservation in early gastric cancer. Sentinel lymphatic pelvic dissection and digital imaging software [103], both of which can reduce false-negative SN fluorescence due to sampling errors or jump metastases, deserve further attention. For lymph node navigation in gastric cancer, no large-scale clinical studies have reported the existence of fluorophores with utility superior to ICG.

5. New advances in fluorescence imaging techniques specifically targeting tumours in peritoneal metastases

Peritoneal dissemination (PD) of abdominal malignancies is the most common form of metastasis from gastric cancer, and its presence portends a poor prognosis. The REGATTA trial reported poor outcomes for unresectable GC, such as peritoneal carcinomatosis, metastasized by gastrectomy [106]. A more thorough evaluation of the spread of this disease is challenging due to the small size of the metastatic lesions and the complexity of the peritoneal cavity.

Fluorescence-guided cytoreduction is one of the most promising methods for eliminating tumours and thus improving prognosis. Intraoperative near-infrared NIR visualization with indocyanine green ICG can improve the diagnostic accuracy of peritoneal metastasis, but NIR-ICG has a limited role in decision-making for peritoneal metastasis in gastric cancer, and its sensitivity and specificity are not satisfactory (sensitivity 86.3 %, specificity 54.2 %) [107], especially for patients with intra-abdominal fibrosis after neoadjuvant therapy. However, ICG-NIR is still an effective complementary tool for laparoscopy (22 % improvement in peritoneal metastasis detection rate) for the purpose of tumour staging [108], or resection of peritoneal metastasis [109].

Detecting peritoneal metastasis is a challenge for fluorescence imaging technology: firstly, there is a lack of truly reliable fluorescent agent. Traditional agent such as ICG injection have poor reproducibility. Several studies have suggested that intraperitoneal injection is superior to intravenous injection for fluorescence detection of peritoneal metastasis [110,111], as repeated injections lead to contamination of the field of view, and ICG is unable to take into account the simultaneous visualization of the primary tumour, lymph node visualization, and peritoneal metastasis. The next issue is how to avoid the interference of fibroblasts on normal or tumour tissues, and another thing that cannot be ignored is the heterogeneity of the study. Based on the current study, it is difficult to derive the overall efficiency of fluorescence detection of peritoneal metastases [112], because so the studies use different protocols: type of fluorescent agent, method of injection, imaging equipment, arterial model, evaluation methods (including in vitro evaluation, evaluation of isolated specimens), and are also affected by tumour heterogeneity.

Detection of peritoneal metastases is not easy due to the lack of biomarkers. Imaging strategies by radiometallic labeling of highly specific antibodies are generally used for preoperative diagnostic imaging of gastric tumours. Intraoperative imaging strategies mainly utilize fluorescent imaging probes, mostly assemblies containing peptide or enzymatic probes, which can specifically diagnose gastric cancer-associated antigens and visualize them with a high tumour background ratio. However, similar studies are largely in the preclinical stage. Another research direction of molecular probes in peritoneal metastasis of gastric cancer is to guide the treatment of intraoperative or postoperative metastases, such as magnetic hyperthermia therapy (MHT), near-infrared photoimmunotherapy (NIR-PIT), and photothermal-enhanced chemotherapy [115–117].

We briefly summarize here some potential intraoperative methods for detecting peritoneal metastases from gastric cancer.

5.1. *Cancer stem cell marker LGR5*

Moon Hwa Kwak [122] developed a peptide probe (IPQILSI) that binds specifically to gastric cancer cells by phage display method for LGR5 in animal models and in vitro experiments. By targeting cancer stem cells to bind specifically to gastric cancer cells, the targeting activity is three times higher than that of normal cells. Not only that, the adhesion ability of IPQILSI to the gastric cancer cell set is much higher, with significantly higher fluorescence observed only in tumour tissues and metastatic tumour tissues, and almost undetectable fluorescence in fibroblasts. These peptide probes are suitable for intraoperative intraperitoneal injection, have good stability, rapid peak absorption and fast clearance, easily penetrate into deep tumour tissues, and they can be reused as they have a low risk of triggering an immune response.

5.2. *β-Galactosidase*

Activatable fluorescent probes targeting cancer-related enzymes are originally non-fluorescent and undergo an enzymatic reaction that significantly increases fluorescence intensity within a few minutes, thus activating the fluorescent probes by simply spraying them locally on the lesion. This type of characterization is highly specific and requires the selection of a specific target enzyme for the type of cancer. So far there are few reports on suitable target enzymes and fluorescent probes for detecting peritoneal metastasis of gastric cancer. Activity of β-Galactosidase (β-Gal) in GC peritoneum is higher than that in normal peritoneum. Hidemasa Kubo [112] demonstrated by cell lines, mouse peritoneal metastasis models, and human GC samples that the SPiDER-βGal probe (an enzyme-activated probe for detecting lymph node metastasis of ovarian cancer) can be used for fluorescence imaging of gastric cancer with the advantages of convenience and non-invasiveness. However, a major limitation faced by enzymatic probes is that consistent enzyme activity cannot be guaranteed in metastatic and primary tumours, and the effect on peritoneal metastasis needs to be studied with more samples.

5.3. Matrix metalloproteinase-14

Another strategy is the complementation of multiple enzymatic probes to improve sensitivity. MMP-14 is a zinc-dependent protein involved in the degradation of the basement membrane and extracellular matrix in gastric cancer, which is an important factor in gastric cancer invasion and metastasis. Soichiro Ogawa developed a targeted MMP-14 probe, BODIPY-MMP [113], for effective application of multi-targeted fluorescence imaging because MMP-14 expression does not correlate with β-Gal activity. Zinc deficiency may affect MMP-14 expression, which may be related to the association between MMP-14 and gastric cancer, whereas zinc levels are affected by age, which was not validated for enzymatic activity in this study.

5.4. Self-assembled peptide nano-chains

The presence of more non-vascularized microtumors (less than 1 mm in diameter) in peritoneal metastases is different from other tumour tissue sites that are well vascularized, which can achieve preferential accumulation of nanoparticles through enhanced permeability and retention (EPR) effects. There are two strategies to address this problem: one is a non-EPR-dependent route of administration, such as the aforementioned intraperitoneal injection. The second is to improve the labeling efficiency of cancer cells and increase the ability to bind molecules, and modulation of the binding capacity between the nanoprobes and the cell membranes is also a promising fluorescence strategy. Qiuxiang Wen [114] designed APP-Ag2S-RGD, which altered the structure of Ag2S-RGD nanoprobes by self-assembling the amphiphilic peptide APP into a nanostrand structure. Due to its flexible geometry and multivalent targeting ability, the probe showed unparalleled sensitivity, and after intraperitoneal injection, non-vascularized microscopic tumour metastases as small as to 0.2 mm in diameter can be easily visualized under NIR-II fluorescence imaging guidance. At the same time, APP-Ag2S-RGD has high fluorescence stability, long retention time in tumour tissue (>5 h) and good biocompatibility. APP-Ag2S-RGD is a promising molecular probe for future preoperative diagnosis and intraoperative navigation.

Fluorescence-guided cytoreduction and intraperitoneal perfusion chemotherapy are one of the most promising approaches to eliminate peritoneal metastases and thus improve the prognosis, but peritoneal metastases are different from primary tumours and require new strategies. (1) Molecularly targeted probes in fluorescence modes such as NIR-II (1000–1700 nm), which are able to penetrate deep tissues while possessing a high degree of sensitivity, are the main research direction for fluorescence imaging of peritoneal metastases. (2) Due to the jumping nature of peritoneal metastases and the fact that some patients have received neoadjuvant conversion therapy, intraoperative spraying of fluorescent agents (or intraperitoneal injection) to suspicious lesions is recommended instead of intravenous injection. In conclusion fluorescence detection of peritoneal metastases from gastric cancer has important research potential and may be part of future comprehensive treatment of peritoneal cancer disease, and although there is no widely recognised method of fluorescence imaging, a growing number of published studies and animal studies indicate interest in this technique.

6. Preclinical study of tumour-targeted fluorescence imaging

The disadvantages of conventional fluorescent tracers, including ICG and methylene blue, include inhomogeneous signals dependent on tumour grading, lack of penetration depth, and photobleaching, and thus structural and functional fluorescence imaging has shifted to molecular fluorescence imaging in recent years. These targeted tracers consist of carrier molecules (e.g. antibodies, peptides or small molecules) and fluorescent probes attached against specific tumour biomarkers. The specific accumulation of the fluorescent contrast agent in the target tissue requires stable binding of the fluorophore to the targeting molecule. As a result, the target cells (most commonly cancer cells) will actually fluoresce, while the background fluorescence is expected to decrease significantly once the unbound tracer is cleared. Clinical translation of targeted fluorescence imaging is often affected by factors such as the chemical properties of the dye, photophysical properties, and tracer attachment difficulties.

Several preclinical studies have demonstrated the great potential of molecular probes. Cristina A. et al. [124] performed fluorescence-guided surgery using fluorophore-conjugated carcinoembryonic antigen antibodies in 73 orthotopic mouse models of human pancreatic cancer, which highlights the tumour, improve surgical resection and increase survival. Orthotopic human pancreatic cancer xenografts were established in nude mice by direct surgical implantation of tumour fragments from fluorescent BxPC-3-RFP subcutaneous tumours. Fluorescence-guided surgery (FGS) was then performed, which resulted in a significant increase in R0 resection rate (45.5 % vs. 92 %, $p = 0.001$), 1-year postoperative survival (0 % vs. 28 %, $p = 0.01$), and median survival (5 weeks vs. 22 weeks, $p = 0.001$) in the FGS group as compared to the bright light surgery (BLS) group. Similar results were obtained in green fluorescent protein (GFP) or red fluorescent protein (RFP)-labelled in orthotopic mouse models of human pancreatic/colon cancer [125,126], and the targeted-tumour imaging techniques were able to translate increased resection rates and reduced tumour recurrence into an overall survival advantage.

Targeted optical fluorescence imaging is rapidly evolving and expanding into clinical applications. Panitimumab-800CW, a probe targeting the epidermal growth factor receptor (EGFR), has been reported in several clinical studies to have a sensitivity of approximately 89 % and a negative predictive value (NPV) of more than 90 % during tumour mapping in head and neck tumour surgery, and panitimumab-800CW was also able to differentiate between low and high levels of fluorescent histopathological dysplasia [127–130]. In addition, in vitro optical fluorescence specimen imaging of panitimumab-800CW is thought to reduce sampling errors in tissue selection for frozen section analysis. However, most of the targeted molecular tracers for gastric cancer are in the preclinical stage, and no clinical studies with large samples have been reported.

Molecular probes play an encouraging role in various aspects of diagnostic tumour imaging, endoscopy, drug therapy, surgical real-

time imaging, and photoimmunotherapy (PIT). Here we only discuss some preclinical studies on the application of some novel probes or strategies in surgical real-time imaging of gastric cancer.

6.1. Carcinoembryonic antigen

Gastric cancer is a highly heterogeneous tumour, and molecular probes constructed on the basis of gastric cancer-specific antibodies, such as EGFR, MG7, VEGF, HER2, are all likely to have varying degrees of false-negative rates if applied in the clinic. The current state of research is that gastric cancer cell lines expressing specific antibodies are mostly selected for imaging in in vitro experiments, while in vivo experiments still lack sufficient immunohistochemical (IHC) data for comparison.

The carcinoembryonic antigen (CEA) is the target with the most clinical translational potential. This 200 kDa glycoprotein is overexpressed in most gastrointestinal and other epithelial tumours. SGM-101 is a mAb-fluorescent conjugate against CEA, in which the near-infrared fluorochrome BM-104 is covalently conjugated to a chimeric monoclonal antibody against carcinoembryonic antigen (CEA), which has an absorbance band centred at 700 nm [131], which has an absorbance band centred on 700 nm, and is suitable for the unambiguous delineation of the tumours. The optical property and stability of SGM-101 make it an excellent candidate for real-time intraoperative tumour imaging. Currently, anti-carcinoembryonic antigen (SGM-101) in combination with IR700 dye is being used to perform fluorescence-guided surgery for colorectal cancer, with promising clinical applications. The phase I/II studies have shown tumour fluorescence in 30 out of 37 patients, with tumour-background ratios (TBR) ranging from 1.5 to 2.4. In addition, have shown tumour fluorescence in 30 out of 37 patients, with tumour-background ratios (TBR) ranging from 1.5 to 2.4. In addition, it effectively binds to human CEA-expressing cells in several mouse models [133].

The safety of molecular probes has always been a concern, and Framery et al. [132] conducted a safety study on SGM-101. As none of the animal species commonly used in toxicological studies express CEA, there are no relevant species to assess the toxicity profile of anti-CEA antibodies or conjugates such as SGM-101. The use of transgenic mice expressing human CEA [132] for toxicological studies was considered inappropriate because the effects associated with the presence of the transgene and/or its expression have not been properly characterised. Therefore, the authors' preclinical toxicological evaluation of SGM-101 was limited to studying the effects of acute intravenous administration in rats, which is consistent with the intended clinical use, as patients will receive a single intravenous administration prior to surgery. Firstly, no signs of toxicity were observed with SGM-101 at a dose of 140 times the maximum expected clinical exposure in Wistar rats and it was not mutagenic in the Ames test. Second, in vitro stability studies in human plasma at 37 °C confirmed the stability of the amide bond between the SGM-101 fluorochrome and the antibody. Third, a toxicokinetic evaluation demonstrated that plasma levels of SGM-101 increased almost proportionally with increasing amounts of SGM-101 injection. Finally, the potential toxicity of the BM-104 dye and the cross-reactivity of SGM-101 were evaluated in 42 human tissues. Even at doses of SGM-10 well above the expected maximum human exposure, no significant adverse reactions were observed. The current clinical trial will continue to evaluate the efficacy of SGM-101 in the detection of small tumour nodules of GI origin and to select the optimal dose for GI tumour detection.

Kristin E. et al. demonstrated that a human carcinoembryonic antigen (M5A) conjugated to a near-infrared dye could selectively label human gastric cancer with high brightness in mouse models [134]. Strong labelling of intra-abdominal and abdominal wall metastases were also observed. Using the surgical orthotopic implantation technique, the authors demonstrated that the M5A-IRDye800CW could detect metastases as small as 2 mm and the use of near-infrared wavelength dyes (700–800 nm) increased the depth of tissue penetration. In addition, peak TBR was reached 72h after injection (ranging from 6.37 to 8.85). Finally, tumour shrinkage by two thirds was achieved by photo-immunotherapy of metastases. This is the first description of a tumour-specific imaging agent for use in an orthotopic mouse model of gastric cancer.

However, a limitation of the study was the use of a single human cancer cell line, which could theoretically produce a homogeneous cell population. Future studies will include the use of patient-derived gastric cancer cells to determine whether anti-carcinoembryonic antigen antibodies brightly target is broadly applicable to primary and metastatic gastric cancer and to determine its potential to mark lymph node metastasis.

6.2. Sandwiched plasmonic biosensor

Most reported NIR-II fluorophores suffer from severe off-target organ retention and/or slow elimination, in addition to the inability of NIR-II imaging to provide quantitative information, which severely hinder its potential clinical application in humans. The authors developed a rapid label-free immunoassay called sandwiched plasmonic chip (SPC) [135]. It employs a novel thickness-sensing mechanism whereby by varying the thickness of the immunoconjugated antibody layer (cetuximab and epidermal growth factor receptor in this study) between gold nanoparticles (NPs) and a printed gold film, the weakening of the electromagnetic coupling between the metallic materials can be converted into a reflected visible light output signal. Thus, the SPC platform with a thickness-sensing mechanism enables high-throughput antibody screening and rapid detection of micrometastatic tumour biomarkers. In this system, the NIR-II navigation system greatly improves the effectiveness of FGS-based tumour therapy by providing precise dissection and identification of tumour-positive lymph nodes. The SPC platform also provides an unprecedented quantitative assessment of target expression for fluorescence-guided surgical systems, opening up new perspectives for preoperative, intraoperative or postoperative diagnosis.

The study is in the preclinical stage and preliminary in vivo studies in mice show potential. The authors chose BFC6TP, a bright and stable NIR-II dye that indiscriminately labels tumours and lymph nodes. BFC6TP outperforms FDA-approved near-infrared fluorophores (ICGs) in identifying tumour-adjacent SLNs and in imaging-guided SLN resection. The visible reflected light signals generated

by SPCs are readily detected by a wide range of visible light readout devices. The process of fabricating the SPC platform is is relatively easy and cost-effective, as only 5 nL of antibody is required to fabricate each SPC spot using a microarray printer. In addition, SPCs have label-free, high-throughput quantification capabilities, and next-generation SPCs hold the promise of integrating a large number of well-known cancer targets across a wide range of cancer types.

6.3. Tumour-associated glycans

Aberrant glycosylation of proteins and lipids is considered to be a hallmark of cancer [136], and some of these antigens, such as sLea and sLex, appear to be largely involved in tumour progression, invasion and metastasis, whereas their roles in healthy tissues are minimal [137]. Tracers to tumour-associated glycans can target multiple tumour-associated proteins and lipids simultaneously, providing a broader range of tumour-targeting strategies than targeting each tumour marker protein individually. Recently Chua et al. developed the novel anti-LecLex, di-Lea, LeaLex, and Lea IgG mouse-derived antibody FG88.2, which showed specific immunohistochemical staining of GI tumour tissues, including gastric carcinoma, while binding to normal tissues was limited [138]. Houvast et al. validated the concept of glycan-based real-time imaging of gastrointestinal tumours using CH88.2 conjugated to the near-infrared fluorophore IRDye800CW, which is a mouse/human chimeric derivative [139]. The authors confirmed specific binding of the antibody on human gastrointestinal tissues and a range of gastrointestinal cell lines, and the specificity of the tracer was assessed in vivo by subcutaneous inoculation of gastric cancer cells in female BALB/c-Nude mice. Gastrointestinal tumours remained clearly demarcated 168 h after IRDye800CW-CH88.2 injection, while the optimal imaging time point under the NIR system was 9 h. Ex vivo analysis of tumour specimens at 1 week post-injection demonstrated that CH88.2–800CW completely penetrated tumours and preserved a high level of fluorescent signal as well as tumour uptake. The TBR of imaging performed with CH88.2–800CW was 2–3 times higher than that imaged with either 800CW or rituximab-800CW, which suggests that CH88.2 specifically binds to make tumours to be easily distinguished from healthy gastrointestinal tissue.

Limitations of this study are that the TBR may be overestimated as mice do not naturally express Lea/c/x glycans, and furthermore, the study did not assess Lea/c/x expression in positive lymph nodes and metastases.

In conclusion, Lewis glycan-based tumour imaging has the advantages of high specificity, wide range of tumour types targeted, long imaging retention time and clear borders, but there is a lack of preclinical studies on lymph nodes and metastatic lesions. Since the tracer consists of a chimeric mAb and an FDA-approved near-infrared fluorescent dye, it provides a new idea for conducting relevant clinical studies.

6.4. Bioorthogonal chemistry

Almost all targeting probes require covalent attachment of targeting molecules (e.g., peptides, antibodies, DNA/RNA aptamers) to NIR fluorophore molecules (e.g., organic dyes) using various bioconjugation strategies. However, NIR fluorophores are relatively large molecules (~1 kDa) that may greatly affect the stereoconformation of the tumour targeting molecules, resulting in the binding affinity and bioavailability of the targeting probe, reducing the sensitivity of the assay and shortening the retention time of the probe in the tumour. In addition, in order to achieve highly sensitive tumour detection, high doses of targeted probes are traditionally required, which inevitably produce toxicity.

It has proposed a new strategy using pre-targeting and bioorthogonal conjugation chemistry [140], also known as the "click chemistry" approach. The probe consists of two click chemistry-mediated components: 1) the pre-labelling agent GEBP11-TCO, either GEBP11 or trans-cyclooctene (TCO), both of which are proven to be highly efficient and sensitive targeting and imaging biomolecules in gastric cancer, and 2) the near-infrared fluorescent agent cyano-5.5 (Cy5.5). The targeted structural domain molecule (GEBP11-TCO) was first injected into the mammalian system to localize it in the target organ and remove it from the non-target organ. The fluorescent coupling agent (Cy5.5-Tz) is then systematically delivered and conjugated to the target structural domains in a highly selective manner via a rapid bioorthogonal chemical reaction. Compared to conventional covalently bonded probes (e.g. GEBP11-Cy5.5), "click chemistry"-mediated probe accumulation in tumours was 11 times higher than with directly labelled probes, tracking lifetime was 12 times longer, and probe uptake in the kidneys was reduced by a factor of 6.5. For diseased tumours of different sizes, click chemistry-mediated probes can achieve sufficient signal-to-noise ratios (3.5–5) for in vivo detection, with a diagnostic sensitivity approximately 3.5 times that of conventional labelled probes. Click chemistry-assisted detection strategies take advantage of "small molecule" probes without interfering with their physiological functions, resulting in highly sensitive and specific-selective tumour detection.

The introduction of smaller "click-chemistry" moieties (<0.2 kDa) into the targeting structural domains and fluorescent partners greatly reduces interference with the binding affinity of specific targeting factors and even improves their binding efficiency. This strategy can provide a readout system with low background and high signal output. The strategy holds promise for overcoming the barriers that limit the effectiveness of conventional coupling methods and may lead to more efficient targeting, longer probe retention times and higher detection sensitivity.

6.5. Molecular imaging of perigastric lymph nodes

As mentioned previously, preoperative and intraoperative diagnosis of lymph nodes (LNs) metastasis in gastric cancer patients is crucial for determining the extent of LN resection as well as for the development of individualised treatment strategies, and a number of novel molecular tracers have initially shown great potential in animal models.

The Lapland-cholesterol nanoprobe "near-infrared polygel" (NIR-PNG) conjugated to IRDye900 demonstrated ideal properties as a surgical tracer for sentinel lymph node navigation [141], as it stays in the sentinel lymph node and does not move to the contiguous distal lymph nodes, a property that can minimize "false" sentinel lymph nodes, and reduce the additional effort and time required to assess lymph nodes. This feature minimises "false" sentinel lymph nodes and reduces the extra effort and time required to assess lymph nodes. Compared to ICG, the properties of NIR-PNG appear to support widespread injections prior to surgery and result in more consistent sentinel lymph node mapping. The results of this study also illustrated that the accuracy of sentinel lymph node detection correlates not only with the sensitivity of the fluorophore, but also with the variability of the retention time of the fluorophore in the sentinel lymph node versus the peripheral lymph node.

IRDye® 800BK, as a hydrophilic fluorophore, can be suitable for the simultaneous visualization of the bile ducts, ureters and perigastric lymph nodes, and is therefore suitable for fluorescence-guided procedures in the gastrointestinal tract. Al-Taher el al. evaluated gastric lymph node visualization and intestinal perfusion in porcine models using IRDye® 800BK [142]. The authors injected 0.6 mg of IRDye® 800BK intravenously into female pigs and found a significant increase in the time to peak (TTP) of IRDye® 800BK in the ischaemic region compared to ICG ($p < 0.039$), which suggests that IRDye® 800BK has a reduced diffusion capacity in the less perfused region, possibly due to the higher molecular weight of this dye compared to ICG. In addition, when 0.6 mg of IRDye® 800BK was injected into the porcine gastric mucosa, the corresponding lymph nodes were clearly identified by NIR fluorescence imaging within 5 min.

Recent advances in nano-based drug delivery systems (DDSs) carriers have facilitated the integration of the diagnostic and therapeutic functions of therapeutic nanoparticles, enabling simultaneous diagnosis, treatment and monitoring of therapeutic response. Tsujimoto et al. established a therapeutic photosensitive nanoparticle [143], which is a micelle assembled from poly (sarcosine)-poly (leuco-lactic acid) (PS-PLLA) block copolymers containing an indocyanine green (ICG) derivative ICG-loaded lactosome (ICGm). The authors injected MKN45 into the hindfoot pads of mice and obtained a popliteal lymph node drainage model 3 weeks later, then injected ICG or ICGm via the tail vein. The metastatic popliteal lymph nodes (simulation of gastric cancer-draining lymph node metastasis) could be clearly detected in ICGm-treated mice but not in ICG-treated mice, and contralateral (non-metastatic) lymph nodes were undetectable in both groups of mice. ICGm, with a diameter of 40–50 nm. Selectively accumulates in tumour tissue via the EPR effect and may be an ideal photosensitiser for the diagnosis and treatment of metastatic lymph nodes.

Tumour-specific fluorescent antibodies can be identified at the cellular or tissue level by optical imaging techniques such as confocal laser endoscopy (CLE), providing a means of rapid and accurate tumour diagnosis and staging. CLE imaging requires the injection of fluorophores (e.g., sodium fluorescein) with wavelengths ranging from 458 nm to 633 nm. One study evaluated the ability of CLE to detect the presence of labelled tumour cells within lymph nodes in a simulated gastric metastatic lymph node model [144]. An indocyanine green solution containing a suspension of porcine hepatocytes (labelled with carboxyfluorescein-succinimidyl ester (CFSE)) was injected endoscopically into the submucosa of the pig's stomach. Fluorescent lymphography was performed using near-infrared laparoscopy to identify anterior and secondary drainage nodes. Two Cellvizio probes, the GastroFlex UHD probe (probe-based CLE, pCLE) and the AQ Flex 19 (niche-based CLE, nCLE) confocal microprobe were used for the study, and 36 lymph nodes were evaluated by IHC and CLE scans, with IHC and CLE concordance of respectively was 83.3 % (pCLE) and 72 % (nCLE). Both modes of CLE were able to detect micrometastases of 0.2–2 mm, but the depth of analysis was higher in nCLE than in pCLE, showing lymphoid tissue and intranodal lymphatic channels in greater detail. The pCLE identifies positive lymph nodes with a borderline distribution, whereas nCLE may be more applicable in the case of a high distribution of positive lymph nodes in the center of the tumour. This study explores the potential of cancer-specific fluorescent antibodies through this original non-cancer model, which is reproducible and modular: various tumour cell lines can be injected into the submucosal layer of the GI tract along with a dye substance to migrate into regional lymph nodes, allowing for testing of lymph node navigation techniques or advanced optical imaging systems. Hepatocytes were chosen because of their ease of collection in large numbers and their ability to be distinguished from lymphoid tissue by IHC. Although CLE has only been reported for the detection of surgically isolated tissue [145], the complete internal structure of the lymph nodes can be clearly visualized by CLE section scanning, independent of the size of the lymph nodes. The novel integration of fluorescently labelled antibodies and confocal laser endoscopy for the rapid visualization of the footprint of dynamic molecules shows improved sensitivity and specificity.

To date, fluorescence molecular imaging has demonstrated its potential to support gastric cancer surgery as well as its feasibility to improve clinical outcomes, but intraoperative fluorescence molecular imaging is now at a critical turning point where definitive efficacy studies are needed to move the field beyond current proof-of-concept studies to make real benefits in clinical practice.

7. Conclusions

Determining a good blood supply to the anastomosis, improving the metastatic lymph node clearance rate, and minimizing collateral damage are essential for the surgical management of gastric cancer patients, while improving the diagnosis of peritoneal metastases of gastric cancer and developing appropriate treatment strategies should also be of continuous interest. Conventional visual fluorescence evaluation in the near-infrared has limited value for the prevention of anastomotic leak, and quantitative assessment methods relying on special software or the application of more camera systems in a minimally invasive setting may be two directions of development in this field.

Fluorescence-guided lymph node dissection, relying on traditional visual fluorescence methods, seems to be applicable only to early gastric cancers, while lymph node navigation in progressive gastric cancers suffers from a non-negligible false-negative rate. Due to the specificity and complexity of lymph node drainage and lymphatic vessel blockage, the application of nonspecific fluorophores in this field has great limitations. The tumour-specific probes that target tumours are still some way from clinical validation.

In addition, imaging strategies specific to overexpression of certain antigens in gastric cancer allow for high contrast display of primary tumours and metastases. The detection of peritoneal metastasis of gastric cancer by fluorescence is a very promising field, but the design of molecular probes is still in the stage of animal experiments, and there is still a certain distance from clinical translation. The field of molecular probes faces greater challenges, such as the toxicity of molecular probes, the heterogeneity of tumour cells, the compatibility of imaging systems and software, and expensive development costs.

Funding

This work was supported by the Social development project of key R&D plan of Department of Science and Technology of Jiangsu Province (BE2022773).

Additional information

No additional information is available for this paper.

Data availability statement

Data availability is not applicable to this article as no new data were created or analyzed in this study.

CRediT authorship contribution statement

Zhu Liu: Writing – review & editing, Writing – original draft, Validation, Supervision, Resources, Investigation, Conceptualization. **Muhammad Ali:** Writing – review & editing. **Qiannan Sun:** Writing – review & editing. **Qi Zhang:** Writing – review & editing, Writing – original draft. **Chen Wei:** Resources. **Yong Wang:** Writing – review & editing, Writing – original draft. **Dong Tang:** Writing – review & editing, Writing – original draft, Supervision, Funding acquisition. **Xin Li:** Writing – review & editing, Writing – original draft, Supervision.

Declaration of competing interest

The authors declare that they have no known competing financial interests or personal relationships that could have appeared to influence the work reported in this paper.

Acknowledgements

The authors would like to thank the Yangzhou Key Laboratory of Basic and Clinical Transformation of Digestive and Metabolic Diseases for providing financial support and technical guidance.

References

[1] H. Sung, J. Ferlay, R.L. Siegel, et al., Global cancer statistics 2020: GLOBOCAN estimates of incidence and mortality worldwide for 36 cancers in 185 countries, CA Cancer J Clin 71 (3) (2021) 209–249.
[2] K. Mabe, K. Inoue, T. Kamada, K. Kato, M. Kato, K. Haruma, Endoscopic screening for gastric cancer in Japan: current status and future perspectives, Dig. Endosc. 34 (3) (2022) 412–419.
[3] A. Petrillo, L. Pompella, G. Tirino, et al., Perioperative treatment in resectable gastric cancer: current perspectives and future directions, Cancers 11 (3) (2019) 399.
[4] C. Egloff-Juras, L. Bezdetnaya, G. Dolivet, H.P. Lassalle, NIR fluorescence-guided tumor surgery: new strategies for the use of indocyanine green, Int J Nanomedicine 14 (2019) 7823–7838. Published 2019 Sep. 25.
[5] H.L. Stewart, D.J.S. Birch, Fluorescence guided surgery, Methods Appl. Fluoresc. 9 (4) (2021), https://doi.org/10.1088/2050-6120/ac1dbb. Published 2021 Aug 26.
[6] D. Ribero, F. Mento, V. Sega, D. Lo Conte, A. Mellano, G. Spinoglio, ICG-guided lymphadenectomy during surgery for colon and rectal cancer-interim analysis of the GREENLIGHT trial, Biomedicines 10 (3) (2022) 541. Published 2022 Feb 24.
[7] P. De Nardi, U. Elmore, G. Maggi, et al., Intraoperative angiography with indocyanine green to assess anastomosis perfusion in patients undergoing laparoscopic colorectal resection: results of a multicenter randomized controlled trial, Surg. Endosc. 34 (1) (2020) 53–60.
[8] J.H. Kim, M. Ku, J. Yang, H.K. Byeon, Recent developments of ICG-guided sentinel lymph node mapping in oral cancer, Diagnostics 11 (5) (2021) 891.
[9] M. Inokuchi, S. Otsuki, Y. Fujimori, Y. Sato, M. Nakagawa, K. Kojima, Systematic review of anastomotic complications of esophagojejunostomy after laparoscopic total gastrectomy, World J. Gastroenterol. 21 (32) (2015) 9656–9665.
[10] A. Karliczek, N.J. Harlaar, C.J. Zeebregts, T. Wiggers, P.C. Baas, G.M. van Dam, Surgeons lack predictive accuracy for anastomotic leakage in gastrointestinal surgery, Int. J. Colorectal Dis. 24 (5) (2009) 569–576.
[11] G. Pavone, A. Fersini, M. Pacilli, P. Cianci, A. Ambrosi, N. Tartaglia, Anastomotic leak test using indocyanine green during laparoscopic Roux-en-Y gastric bypass: a cohort study, Ann Med Surg (Lond). 84 (2022) 104939. Published 2022 Nov 17.
[12] M.D. Jafari, S.D. Wexner, J.E. Martz, et al., Perfusion assessment in laparoscopic left-sided/anterior resection (PILLAR II): a multi-institutional study, J. Am. Coll. Surg. 220 (1) (2015) 82–92.e1.
[13] F. Ris, E. Liot, N.C. Buchs, et al., Multicentre phase II trial of near-infrared imaging in elective colorectal surgery, Br. J. Surg. 105 (10) (2018) 1359–1367.
[14] M. Mori, K. Shuto, A. Hirano, et al., A novel parameter identified using indocyanine green fluorescence angiography may contribute to predicting anastomotic leakage in gastric cancer surgery, World J. Surg. 44 (8) (2020) 2699–2708.

[15] C.A. Nwaiwu, V.E. Buharin, A. Mach, et al., Feasibility and comparison of laparoscopic laser speckle contrast imaging to near-infrared display of indocyanine green in intraoperative tissue blood flow/tissue perfusion in preclinical porcine models, Surg. Endosc. (2022), https://doi.org/10.1007/s00464-022-09583-2 [published online ahead of print, 2022 Sep 16].

[16] N. Nerup, M.B.S. Svendsen, J.H. Rønn, L. Konge, L.B. Svendsen, M.P. Achiam, Quantitative fluorescence angiography aids novice and experienced surgeons in performing intestinal resection in well-perfused tissue, Surg. Endosc. 36 (4) (2022) 2373–2381.

[17] S.R. Thammineedi, S.C. Patnaik, A.R. Saksena, P.R. Ramalingam, S. Nusrath, The utility of indocyanine green angiography in the assessment of perfusion of gastric conduit and proximal esophageal stump against visual assessment in patients undergoing esophagectomy: a prospective study, Indian J Surg Oncol 11 (4) (2020) 684–691.

[18] E. Talavera-Urquijo, P. Parise, M. Palucci, et al., Perfusion speed of indocyanine green in the stomach before tubulization is an objective and useful parameter to evaluate gastric microcirculation during Ivor-Lewis esophagectomy, Surg. Endosc. 34 (12) (2020) 5649–5659.

[19] N.P. Hardy, J.J. Joosten, J. Dalli, R. Hompes, R.A. Cahill, M.I. van Berge Henegouwen, Evaluation of inter-user variability in indocyanine green fluorescence angiography to assess gastric conduit perfusion in esophageal cancer surgery, Dis. Esophagus 35 (11) (2022) doac016.

[20] D.A. Sherwinter, J. Gallagher, T. Donkar, Intra-operative transanal near infrared imaging of colorectal anastomotic perfusion: a feasibility study, Colorectal Dis. 15 (1) (2013) 91–96.

[21] Y.J. Huh, H.J. Lee, T.H. Kim, et al., Efficacy of assessing intraoperative bowel perfusion with near-infrared camera in laparoscopic gastric cancer surgery, J. Laparoendosc. Adv. Surg. Tech. 29 (4) (2019) 476–483.

[22] K. Koyanagi, S. Ozawa, J. Oguma, et al., Blood flow speed of the gastric conduit assessed by indocyanine green fluorescence: new predictive evaluation of anastomotic leakage after esophagectomy, Medicine (Baltim.) 95 (30) (2016) e4386.

[23] K. Koyanagi, S. Ozawa, Y. Ninomiya, et al., Association between indocyanine green fluorescence blood flow speed in the gastric conduit wall and superior mesenteric artery calcification: predictive significance for anastomotic leakage after esophagectomy, Esophagus 18 (2) (2021) 248–257.

[24] Y. Kumagai, S. Hatano, J. Sobajima, et al., Indocyanine green fluorescence angiography of the reconstructed gastric tube during esophagectomy: efficacy of the 90-second rule, Dis. Esophagus 31 (12) (2018), https://doi.org/10.1093/dote/doy052.

[25] P.H. von Kroge, D. Russ, H.C. Rieß, et al., The impact of nitroglycerine and volume on gastric tube microperfusion assessed by indocyanine green fluorescence imaging, Sci. Rep. 12 (1) (2022) 22394. Published 2022 Dec 27.

[26] K. Noma, Y. Shirakawa, N. Kanaya, et al., Visualized evaluation of blood flow to the gastric conduit and complications in esophageal reconstruction, J. Am. Coll. Surg. 226 (3) (2018) 241–251.

[27] K. Pather, A.M. Deladisma, C. Guerrier, I.R. Kriley, Z.T. Awad, Indocyanine green perfusion assessment of the gastric conduit in minimally invasive Ivor Lewis esophagectomy, Surg. Endosc. 36 (2) (2022) 896–903.

[28] B.G.A. Dalton, A.A. Ali, M. Crandall, Z.T. Awad, Near infrared perfusion assessment of gastric conduit during minimally invasive Ivor Lewis esophagectomy, Am. J. Surg. 216 (3) (2018) 524–527.

[29] M.D. Slooter, D.M. de Bruin, W.J. Eshuis, et al., Quantitative fluorescence-guided perfusion assessment of the gastric conduit to predict anastomotic complications after esophagectomy, Dis. Esophagus 34 (5) (2021) doaa100, https://doi.org/10.1093/dote/doaa100.

[30] E. Van Daele, N. De Bruyne, H. Vanommeslaeghe, Y. Van Nieuwenhove, W. Ceelen, P. Pattyn, Clinical utility of near-infrared perfusion assessment of the gastric tube during Ivor Lewis esophagectomy, Surg. Endosc. 36 (8) (2022) 5812–5821.

[31] N. Nerup, M.B.S. Svendsen, L.B. Svendsen, M.P. Achiam, Feasibility and usability of real-time intraoperative quantitative fluorescent-guided perfusion assessment during resection of gastroesophageal junction cancer, Langenbeck's Arch. Surg. 405 (2) (2020) 215–222.

[32] C. Detter, S. Wipper, D. Russ, et al., Fluorescent cardiac imaging: a novel intraoperative method for quantitative assessment of myocardial perfusion during graded coronary artery stenosis, Circulation 116 (9) (2007) 1007–1014.

[33] N. Nerup, H.S. Andersen, R. Ambrus, et al., Quantification of fluorescence angiography in a porcine model, Langenbeck's Arch. Surg. 402 (4) (2017) 655–662.

[34] P. von Kroge, D. Russ, J. Wagner, et al., Quantification of gastric tube perfusion following esophagectomy using fluorescence imaging with indocyanine green, Langenbeck's Arch. Surg. 407 (7) (2022) 2693–2701.

[35] C.D. Lütken, M.P. Achiam, M.B. Svendsen, L. Boni, N. Nerup, Optimizing quantitative fluorescence angiography for visceral perfusion assessment, Surg. Endosc. 34 (12) (2020) 5223–5233.

[36] F. Ishige, Y. Nabeya, I. Hoshino, et al., Quantitative assessment of the blood perfusion of the gastric conduit by indocyanine green imaging, J. Surg. Res. 234 (2019) 303–310.

[37] S.M. Jansen, D.M. de Bruin, L.S. Wilk, et al., Quantitative fluorescence imaging of perfusion-an algorithm to predict anastomotic leakage, Life 12 (2) (2022) 249.

[38] H. Prasetya, S.M. Jansen, H.A. Marquering, et al., Estimation of microvascular perfusion after esophagectomy: a quantitative model of dynamic fluorescence imaging, Med. Biol. Eng. Comput. 57 (9) (2019) 1889–1900.

[39] M. Mori, K. Shuto, A. Hirano, et al., A novel parameter identified using indocyanine green fluorescence angiography may contribute to predicting anastomotic leakage in gastric cancer surgery, World J. Surg. 44 (8) (2020) 2699–2708.

[40] M.S. Maish, S.R. DeMeester, E. Choustoulakis, et al., The safety and usefulness of endoscopy for evaluation of the graft and anastomosis early after esophagectomy and reconstruction, Surg. Endosc. 19 (8) (2005) 1093–1102.

[41] J. Osterkamp, R. Strandby, N. Nerup, M. Svendsen, L. Svendsen, M. Achiam, Quantitative fluorescence angiography detects dynamic changes in gastric perfusion, Surg. Endosc. 35 (12) (2021) 6786–6795.

[42] A. Duprée, H.C. Rieß, P.H. von Kroge, et al., Validation of quantitative assessment of indocyanine green fluorescent imaging in a one-vessel model, PLoS One 15 (11) (2020) e0240188. Published 2020 Nov 18.

[43] R. Ambrus, M.P. Achiam, N.H. Secher, et al., Evaluation of gastric microcirculation by laser speckle contrast imaging during esophagectomy, J. Am. Coll. Surg. 225 (3) (2017) 395–402.

[44] C.A. Nwaiwu, V.E. Buharin, A. Mach, et al., Feasibility and comparison of laparoscopic laser speckle contrast imaging to near-infrared display of indocyanine green in intraoperative tissue blood flow/tissue perfusion in preclinical porcine models, Surg. Endosc. (2022), https://doi.org/10.1007/s00464-022-09583-2 [published online ahead of print, 2022 Sep 16].

[45] N. Nerup, K.B.K. Knudsen, R. Ambrus, et al., Reproducibility and reliability of repeated quantitative fluorescence angiography, Surg. Technol. Int. 31 (2017) 35–39.

[46] Y.Z. Liu, S.K. Shah, C.M. Sanders, et al., Utility and usability of laser speckle contrast imaging (LSCI) for displaying real-time tissue perfusion/blood flow in robot-assisted surgery (RAS): comparison to indocyanine green (ICG) and use in laparoscopic surgery, Surg. Endosc. (2022) 1–9 [published online ahead of print, 2022 Sep 15].

[47] H. Köhler, A. Kulcke, M. Maktabi, et al., Laparoscopic system for simultaneous high-resolution video and rapid hyperspectral imaging in the visible and near-infrared spectral range, J. Biomed. Opt. 25 (8) (2020) 086004.

[48] M. Barberio, F. Longo, C. Fiorillo, et al., HYPerspectral Enhanced Reality (HYPER): a physiology-based surgical guidance tool, Surg. Endosc. 34 (4) (2020) 1736–1744.

[49] S. Hennig, B. Jansen-Winkeln, H. Köhler, et al., Novel intraoperative imaging of gastric tube perfusion during oncologic esophagectomy-A pilot study comparing hyperspectral imaging (HSI) and fluorescence imaging (FI) with indocyanine green (ICG), Cancers 14 (1) (2021) 97. Published 2021 Dec 25.

[50] Y. Ikeda, M. Niimi, S. Kan, T. Shatari, H. Takami, S. Kodaira, Clinical significance of tissue blood flow during esophagectomy by laser Doppler flowmetry, J. Thorac. Cardiovasc. Surg. 122 (6) (2001) 1101–1106.

[51] N. Safi, H.O. Johannessen, A.W. Medhus, T. Mala, S.S.H. Kazmi, Laser Doppler flowmetry and visible light spectroscopy of the gastric tube during minimally invasive esophagectomy, Vasc. Health Risk Manag. 16 (2020) 497–505. Published 2020 Nov 27.

[52] P.M. Kuri, E. Pion, L. Mahl, et al., Deep learning-based image analysis for the quantification of tumor-induced angiogenesis in the 3D in vivo tumor model-establishment and addition to laser speckle contrast imaging (LSCI), Cells 11 (15) (2022) 2321. Published 2022 Jul 28.

[53] S. Takiguchi, Y. Fujiwara, M. Yamasaki, et al., Laparoscopic intraoperative navigation surgery for gastric cancer using real-time rendered 3D CT images, Surg. Today 45 (5) (2015) 618–624.
[54] Y. Hayashi, K. Misawa, D.J. Hawkes, K. Mori, Progressive internal landmark registration for surgical navigation in laparoscopic gastrectomy for gastric cancer, Int. J. Comput. Assist. Radiol. Surg. 11 (5) (2016) 837–845.
[55] M. Kim, S.Y. Son, L.H. Cui, H.J. Shin, H. Hur, S.U. Han, Real-time vessel navigation using indocyanine green fluorescence during robotic or laparoscopic gastrectomy for gastric cancer, J Gastric Cancer 17 (2) (2017) 145–153.
[56] Y. Ebihara, Y. Kurashima, S. Murakami, T. Shichinohe, S. Hirano, Robotic real-time vessel navigation using indocyanine green fluorescence for lymph node dissection along the left gastroepiploic vessels during robotic distal gastrectomy - first experience, J Minim Access Surg 18 (4) (2022) 619–621, https://doi.org/10.4103/jmas.jmas_223_21.
[57] Y. Ebihara, Y. Kurashima, S. Murakami, T. Shichinohe, S. Hirano, Robotic real-time vessel navigation using indocyanine green fluorescence for lymph node dissection along the left gastroepiploic vessels during robotic distal gastrectomy - first experience, J Minim Access Surg 18 (4) (2022) 619–621.
[58] J.H. Lee, T. Son, Y.E. Chung, et al., Real-time identification of aberrant left hepatic arterial territories using near-infrared fluorescence with indocyanine green during gastrectomy for gastric cancer, Surg. Endosc. 35 (5) (2021) 2389–2397.
[59] T. Kamada, H. Ohdaira, K. Nakashima, et al., Real-time vessel navigation using indocyanine green fluorescence during robotic-assisted gastrectomy for gastric cancer after coronary artery bypass grafting using the right gastroepiploic artery [published online ahead of print, 2023 Jan 4], Asian J. Endosc. Surg. (2023), https://doi.org/10.1111/ases.13161.
[60] S. Asari, H. Toyama, T. Goto, et al., Indocyanine green (ICG) fluorography and digital subtraction angiography (DSA) of vessels supplying the remnant stomach that were performed during distal pancreatectomy in a patient with a history of distal gastrectomy: a case report, Clin J Gastroenterol 14 (6) (2021) 1749–1755, https://doi.org/10.1007/s12328-021-01493-5.
[61] S. Kawaguchi, S. Okubo, S. Haruta, J. Shindoh, M. Hashimoto, M. Ueno, Indocyanine green fluorescence angiography-guided simultaneous laparoscopic distal gastrectomy and spleen-preserving distal pancreatectomy for conserving the gastrosplenic ligament: a case report, Int J Surg Case Rep 92 (2022) 106803.
[62] M. Cho, K.Y. Kim, S.H. Park, Y.M. Kim, H.I. Kim, W.J. Hyung, Securing resection margin using indocyanine green diffusion range on gastric wall during NIR fluorescence-guided surgery in early gastric cancer patients, Cancers 14 (21) (2022) 5223. Published 2022 Oct 25.
[63] W.O. de Steur, H.H. Hartgrink, J.L. Dikken, H. Putter, C.J. van de Velde, Quality control of lymph node dissection in the Dutch Gastric Cancer Trial, Br. J. Surg. 102 (11) (2015) 1388–1393, https://doi.org/10.1002/bjs.9891.
[64] J.S. Chang, K.H. Kim, H.I. Yoon, et al., Locoregional relapse after gastrectomy with D2 lymphadenectomy for gastric cancer, Br. J. Surg. 104 (7) (2017) 877–884.
[65] B.W. Eom, J. Joo, Y.W. Kim, et al., Improved survival after adding dissection of the superior mesenteric vein lymph node (14v) to standard D2 gastrectomy for advanced distal gastric cancer, Surgery 155 (3) (2014) 408–416.
[66] S.H. Park, F. Berlth, J.H. Choi, et al., Near-infrared fluorescence-guided surgery using indocyanine green facilitates secure infrapyloric lymph node dissection during laparoscopic distal gastrectomy, Surg. Today 50 (10) (2020) 1187–1196.
[67] M. Wei, Y. Liang, L. Wang, et al., Clinical application of indocyanine green fluorescence technology in laparoscopic radical gastrectomy, Front. Oncol. 12 (2022) 847341.
[68] T.H. Kim, S.H. Kong, J.H. Park, et al., Assessment of the completeness of lymph node dissection using near-infrared imaging with indocyanine green in laparoscopic gastrectomy for gastric cancer, J Gastric Cancer 18 (2) (2018) 161–171.
[69] J.W. Park, D.K. Sohn, C.W. Hong, et al., The usefulness of preoperative colonoscopic tattooing using a saline test injection method with prepackaged sterile India ink for localization in laparoscopic colorectal surgery, Surg. Endosc. 22 (2) (2008) 501–505.
[70] J.H. Park, F. Berlth, C. Wang, et al., Mapping of the perigastric lymphatic network using indocyanine green fluorescence imaging and tissue marking dye in clinically advanced gastric cancer, Eur. J. Surg. Oncol. 48 (2) (2022) 411–417.
[71] Z.N. Huang, Su Yan, W.W. Qiu, et al., Assessment of indocyanine green tracer-guided lymphadenectomy in laparoscopic gastrectomy after neoadjuvant chemotherapy for locally advanced gastric cancer: results from a multicenter analysis based on propensity matching, Gastric Cancer 24 (6) (2021) 1355–1364.
[72] F. Puccetti, L. Cinelli, L. Genova, et al., Applicative limitations of indocyanine green fluorescence assistance to laparoscopic lymph node dissection in total gastrectomy for cancer, Ann. Surg Oncol. 29 (9) (2022) 5875–5882.
[73] X. Chen, Z. Zhang, F. Zhang, et al., Analysis of safety and efficacy of laparoscopic radical gastrectomy combined with or without indocyanine green tracer fluorescence technique in treatment of gastric cancer: a retrospective cohort study, J. Gastrointest. Oncol. 13 (4) (2022) 1616–1625.
[74] Q.Y. Chen, J.W. Xie, Q. Zhong, et al., Safety and efficacy of indocyanine green tracer-guided lymph node dissection during laparoscopic radical gastrectomy in patients with gastric cancer: a randomized clinical trial, JAMA Surg 155 (4) (2020) 300–311.
[75] A. Watanabe, T.D. Hamilton, Lymph node mapping in gastric cancer: a pilot study in Western patients, Can. J. Surg. 65 (5) (2022) E630–E634.
[76] M. Wei, Y. Liang, L. Wang, et al., Clinical application of indocyanine green fluorescence technology in laparoscopic radical gastrectomy, Front. Oncol. 12 (2022) 847341.
[77] S. Lee, J.H. Song, S. Choi, et al., Fluorescent lymphography during minimally invasive total gastrectomy for gastric cancer: an effective technique for splenic hilar lymph node dissection, Surg. Endosc. 36 (5) (2022) 2914–2924.
[78] J. Deng, H. Yamashita, Y. Seto, H. Liang, Increasing the number of examined lymph nodes is a prerequisite for improvement in the accurate evaluation of overall survival of node-negative gastric cancer patients, Ann. Surg Oncol. 24 (3) (2017) 745–753.
[79] K.A. Mirkin, C.S. Hollenbeak, J. Wong, Greater lymph node retrieval improves survival in node-negative resected gastric cancer in the United States, J Gastric Cancer 17 (4) (2017) 306–318.
[80] W.O. de Steur, H.H. Hartgrink, J.L. Dikken, H. Putter, C.J. van de Velde, Quality control of lymph node dissection in the Dutch Gastric Cancer Trial, Br. J. Surg. 102 (11) (2015) 1388–1393.
[81] Q.Y. Chen, J.W. Xie, Q. Zhong, et al., Safety and efficacy of indocyanine green tracer-guided lymph node dissection during laparoscopic radical gastrectomy in patients with gastric cancer: a randomized clinical trial, JAMA Surg 155 (4) (2020) 300–311.
[82] J.Y. Park, K.W. Ryu, B.W. Eom, et al., Proposal of the surgical options for primary tumor control during sentinel node navigation surgery based on the discrepancy between preoperative and postoperative early gastric cancer diagnoses, Ann. Surg Oncol. 21 (4) (2014) 1123–1129.
[83] T. Fujimura, S. Fushida, T. Tsukada, et al., A new stage of sentinel node navigation surgery in early gastric cancer, Gastric Cancer 18 (2) (2015) 210–217.
[84] Y.J. Lee, S.H. Jeong, H. Hur, et al., Prospective multicenter feasibility study of laparoscopic sentinel basin dissection for organ preserving surgery in gastric cancer: quality control study for surgical standardization prior to phase III trial, Medicine (Baltim.) 94 (43) (2015) e1894.
[85] C.M. Lee, S. Park, S.H. Park, et al., Sentinel node mapping using a fluorescent dye and visible light during laparoscopic gastrectomy for early gastric cancer: result of a prospective study from a single institute, Ann. Surg. 265 (4) (2017) 766–773.
[86] I.G. Kwon, T. Son, H.I. Kim, W.J. Hyung, Fluorescent lymphography-guided lymphadenectomy during robotic radical gastrectomy for gastric cancer, JAMA Surg 154 (2) (2019) 150–158.
[87] C.K. Roh, S. Choi, W.J. Seo, et al., Indocyanine green fluorescence lymphography during gastrectomy after initial endoscopic submucosal dissection for early gastric cancer, Br. J. Surg. 107 (6) (2020) 712–719.
[88] S.H. Kong, F. Marchegiani, R. Soares, et al., Fluorescence lymphangiography-guided full-thickness oncologic gastric resection, Surg. Endosc. 33 (2) (2019) 620–632.
[89] T. Arigami, Y. Uenosono, S. Yanagita, et al., Clinical significance of lymph node micrometastasis in gastric cancer, Ann. Surg Oncol. 20 (2) (2013) 515–521.
[90] J.Y. Park, M.C. Kook, B.W. Eom, et al., Practical intraoperative pathologic evaluation of sentinel lymph nodes during sentinel node navigation surgery in gastric cancer patients - proposal of the pathologic protocol for the upcoming SENORITA trial, Surg Oncol 25 (3) (2016) 139–146.
[91] P. Treseler, Pathologic examination of the sentinel lymph node: what is the best method? Breast J. 12 (5 Suppl 2) (2006) S143–S151.
[92] G.H. Lyman, S. Temin, S.B. Edge, et al., Sentinel lymph node biopsy for patients with early-stage breast cancer: American Society of Clinical Oncology clinical practice guideline update, J. Clin. Oncol. 32 (13) (2014) 1365–1383.

[93] K. Miwa, S. Kinami, K. Taniguchi, S. Fushida, T. Fujimura, A. Nonomura, Mapping sentinel nodes in patients with early-stage gastric carcinoma, Br. J. Surg. 90 (2) (2003) 178–182.
[94] Y. Kitagawa, H. Takeuchi, Y. Takagi, et al., Sentinel node mapping for gastric cancer: a prospective multicenter trial in Japan, J. Clin. Oncol. 31 (29) (2013) 3704–3710.
[95] H. Takeuchi, Y. Kitagawa, New sentinel node mapping technologies for early gastric cancer, Ann. Surg Oncol. 20 (2) (2013) 522–532.
[96] K. Yano, H. Nimura, N. Mitsumori, N. Takahashi, H. Kashiwagi, K. Yanaga, The efficiency of micrometastasis by sentinel node navigation surgery using indocyanine green and infrared ray laparoscopy system for gastric cancer, Gastric Cancer 15 (3) (2012) 287–291.
[97] H. Liu, F. Wang, B. Liu, Z. Zheng, J. Zhao, J. Zhang, Application of three-dimensional reconstruction with a Hisense computer-assisted system in upper pancreatic lymph node dissection during laparoscopic-assisted radical gastrectomy, Asian J. Surg. 44 (5) (2021) 730–737.
[98] H. Wang, M.M. Chen, G.S. Zhu, M.G. Ma, H.S. Du, Y.P. Long, Lymph node mapping with carbon nanoparticles and the risk factors of lymph node metastasis in gastric cancer, J Huazhong Univ Sci Technolog Med Sci 36 (6) (2016) 865–870.
[99] Y. Liao, J. Zhao, Y. Chen, et al., Mapping lymph node during indocyanine green fluorescence-imaging guided gastric oncologic surgery: current applications and future directions, Cancers 14 (20) (2022) 5143. Published 2022 Oct 20.
[100] J. Osterkamp, R.B. Strandby, N. Nerup, M.B.S. Svendsen, L.B. Svendsen, M.P. Achiam, Time to maximum indocyanine green fluorescence of gastric sentinel lymph nodes and feasibility of combined indocyanine green/sodium fluorescein gastric lymphography, Langenbeck's Arch. Surg. 406 (8) (2021) 2717–2724.
[101] A. Shida, N. Mitsumori, H. Nimura, et al., Prediction of lymph node metastasis and sentinel node navigation surgery for patients with early-stage gastric cancer, World J. Gastroenterol. 22 (33) (2016) 7431–7439.
[102] T. Tani, H. Sonoda, M. Tani, Sentinel lymph node navigation surgery for gastric cancer: does it really benefit the patient? World J. Gastroenterol. 22 (10) (2016) 2894–2899.
[103] N. Takahashi, H. Nimura, T. Fujita, S. Yamashita, N. Mitsumori, K. Yanaga, Quantitative assessment of visual estimation of the infrared indocyanine green imaging of lymph nodes retrieved at sentinel node navigation surgery for gastric cancer, BMC Surg. 16 (1) (2016) 35. Published 2016 Jun 1.
[104] A. Wildeboer, W. Heeman, A. van der Bilt, et al., Laparoscopic laser speckle contrast imaging can visualize anastomotic perfusion: a demonstration in a porcine model, Life 12 (8) (2022) 1251. Published 2022 Aug 16.
[105] K. Fujitani, H.K. Yang, J. Mizusawa, et al., Gastrectomy plus chemotherapy versus chemotherapy alone for advanced gastric cancer with a single non-curable factor (REGATTA): a phase 3, randomised controlled trial, Lancet Oncol. 17 (3) (2016) 309–318.
[106] S. Boussedra, L. Benoit, M. Koual, et al., Fluorescence guided surgery to improve peritoneal cytoreduction in epithelial ovarian cancer: a systematic review of available data, Eur. J. Surg. Oncol. 48 (6) (2022) 1217–1223.
[107] S. Shirakawa, H. Toyama, M. Kido, T. Fukumoto, A prospective single-center protocol for using near-infrared fluorescence imaging with indocyanine green during staging laparoscopy to detect small metastasis from pancreatic cancer, BMC Surg. 19 (1) (2019) 165.
[108] Y. Tani, H. Sato, R. Yoshida, et al., Favorable control of hepatocellular carcinoma with peritoneal dissemination by surgical resection using indocyanine green fluorescence imaging: a case report and review of the literature, J. Med. Case Rep. 16 (1) (2022) 222.
[109] A. Taibi, J. Albouys, J. Jacques, et al., Comparison of implantation sites for the development of peritoneal metastasis in a colorectal cancer mouse model using non-invasive bioluminescence imaging, PLoS One 14 (7) (2019) e0220360. Published 2019 Jul 31.
[110] T. Sun, G. Zhang, T. Ning, et al., A versatile theranostic platform for colorectal cancer peritoneal metastases: real-time tumor-tracking and photothermal-enhanced chemotherapy, Adv. Sci. 8 (20) (2021) e2102256.
[111] S. Boussedra, L. Benoit, M. Koual, et al., Fluorescence guided surgery to improve peritoneal cytoreduction in epithelial ovarian cancer: a systematic review of available data, Eur. J. Surg. Oncol. 48 (6) (2022) 1217–1223.
[112] H. Kubo, Y. Murayama, S. Ogawa, et al., β-Galactosidase is a target enzyme for detecting peritoneal metastasis of gastric cancer, Sci. Rep. 11 (1) (2021) 10664.
[113] S. Ogawa, H. Kubo, Y. Murayama, et al., Matrix metalloprotease-14 is a target enzyme for detecting peritoneal metastasis in gastric cancer, Photodiagnosis Photodyn. Ther. 35 (2021) 102420.
[114] Q. Wen, Y. Zhang, C. Li, et al., NIR-II fluorescent self-assembled peptide nanochain for ultrasensitive detection of peritoneal metastasis, Angew Chem. Int. Ed. Engl. 58 (32) (2019) 11001–11006.
[115] Y. Matsumi, T. Kagawa, S. Yano, et al., Hyperthermia generated by magnetic nanoparticles for effective treatment of disseminated peritoneal cancer in an orthotopic nude-mouse model, Cell Cycle 20 (12) (2021) 1122–1133.
[116] T. Nagaya, S. Okuyama, F. Ogata, Y. Maruoka, P.L. Choyke, H. Kobayashi, Near infrared photoimmunotherapy using a fiber optic diffuser for treating peritoneal gastric cancer dissemination, Gastric Cancer 22 (3) (2019) 463–472.
[117] Q. Zhong, Q.Y. Chen, X.B. Huang, et al., Clinical implications of Indocyanine Green Fluorescence Imaging-Guided laparoscopic lymphadenectomy for patients with gastric cancer: a cohort study from two randomized, controlled trials using individual patient data, Int. J. Surg. 94 (2021) 106120.
[118] Q.Y. Chen, Q. Zhong, P. Li, et al., Comparison of submucosal and subserosal approaches toward optimized indocyanine green tracer-guided laparoscopic lymphadenectomy for patients with gastric cancer (FUGES-019): a randomized controlled trial, BMC Med. 19 (1) (2021) 276.
[119] C. Sposito, M. Maspero, V. Conalbi, et al., Impact of indocyanine green fluorescence imaging on lymphadenectomy quality during laparoscopic distal gastrectomy for gastric cancer (greeneye): an adaptative, phase 2, clinical trial, Ann. Surg Oncol. 30 (11) (2023) 6803–6811.
[120] Q.R. Tummers, L.S. Boogerd, W.O. de Steur, et al., Near-infrared fluorescence sentinel lymph node detection in gastric cancer: a pilot study, World J. Gastroenterol. 22 (13) (2016) 3644–3651.
[121] K. Nishikawa, T. Fujita, M. Yuda, et al., Quantitative assessment of blood flow in the gastric conduit with thermal imaging for esophageal reconstruction, Ann. Surg. 271 (6) (2020) 1087–1094.
[122] M.H. Kwak, S.M. Yang, S.K. Yun, S. Kim, M.G. Choi, J.M. Park, Identification and validation of LGR5-binding peptide for molecular imaging of gastric cancer, Biochem. Biophys. Res. Commun. 580 (2021) 93–99.
[123] T. Omori, H. Hara, N. Shinno, et al., Safety and efficacy of preoperative indocyanine green fluorescence marking in laparoscopic gastrectomy for proximal gastric and esophagogastric junction adenocarcinoma (ICG MAP study), Langenbeck's Arch. Surg. 407 (8) (2022) 3387–3396.
[124] C.A. Metildi, S. Kaushal, M. Pu, et al., Fluorescence-guided surgery with a fluorophore-conjugated antibody to carcinoembryonic antigen (CEA), that highlights the tumor, improves surgical resection and increases survival in orthotopic mouse models of human pancreatic cancer, Ann. Surg Oncol. 21 (4) (2014) 1405–1411.
[125] C.A. Metildi, S. Kaushal, C.S. Snyder, R.M. Hoffman, M. Bouvet, Fluorescence-guided surgery of human colon cancer increases complete resection resulting in cures in an orthotopic nude mouse model, J. Surg. Res. 179 (1) (2013) 87–93.
[126] C.A. Metildi, S. Kaushal, C.R. Hardamon, et al., Fluorescence-guided surgery allows for more complete resection of pancreatic cancer, resulting in longer disease-free survival compared with standard surgery in orthotopic mouse models, J. Am. Coll. Surg. 215 (1) (2012) 126–136.
[127] R.W. Gao, N.T. Teraphongphom, N.S. van den Berg, et al., Determination of tumor margins with surgical specimen mapping using near-infrared fluorescence, Cancer Res. 78 (17) (2018) 5144–5154.
[128] S. Van Keulen, N. Nishio, A. Birkeland, et al., The sentinel margin: intraoperative ex vivo specimen mapping using relative fluorescence intensity, Clin. Cancer Res. 25 (15) (2019) 4656–4662.
[129] S. Van Keulen, N.S. van den Berg, N. Nishio, et al., Rapid, non-invasive fluorescence margin assessment: optical specimen mapping in oral squamous cell carcinoma, Oral Oncol. 88 (2019) 58–65.
[130] S. Fakurnejad, S. van Keulen, N. Nishio, et al., Fluorescence molecular imaging for identification of high-grade dysplasia in patients with head and neck cancer, Oral Oncol. 97 (2019) 50–55.
[131] M. Gutowski, B. Framery, M.C. Boonstra, et al., SGM-101: an innovative near-infrared dye-antibody conjugate that targets CEA for fluorescence-guided surgery, Surg Oncol 26 (2) (2017) 153–162.
[132] B. Framery, M. Gutowski, K. Dumas, et al., Toxicity and pharmacokinetic profile of SGM-101, a fluorescent anti-CEA chimeric antibody for fluorescence imaging of tumors in patients, Toxicol Rep 6 (2019) 409–415. Published 2019 Apr 30.

[133] P. Clarke, J. Mann, J.F. Simpson, K. Rickard-Dickson, F.J. Primus, Mice transgenic for human carcinoembryonic antigen as a model for immunotherapy, Cancer Res. 58 (7) (1998) 1469–1477.
[134] K.E. Cox, M.A. Turner, S. Amirfakhri, et al., Humanized anti-carcinoembryonic antigen antibodies brightly target and label gastric cancer in orthotopic mouse models, J. Surg. Res. 293 (2024) 701–708.
[135] Y. Wang, J. Nan, H. Ma, et al., NIR-II imaging and sandwiched plasmonic biosensor for ultrasensitive intraoperative definition of tumor-invaded lymph nodes, Nano Lett. 23 (9) (2023) 4039–4048.
[136] S.S. Pinho, C.A. Reis, Glycosylation in cancer: mechanisms and clinical implications, Nat. Rev. Cancer 15 (9) (2015) 540–555.
[137] J. Munkley, The role of sialyl-tn in cancer, Int. J. Mol. Sci. 17 (3) (2016) 275. Published 2016 Feb 24.
[138] J.X. Chua, M. Vankemmelbeke, R.S. McIntosh, et al., Monoclonal antibodies targeting LecLex-related glycans with potent antitumor activity, Clin. Cancer Res. 21 (13) (2015) 2963–2974.
[139] R.D. Houvast, V.M. Baart, S.S. Bhairosingh, et al., Glycan-based near-infrared fluorescent (NIRF) imaging of gastrointestinal tumors: a preclinical proof-of-concept in vivo study, Mol Imaging Biol 22 (6) (2020) 1511–1522.
[140] X. Zhang, B. Wang, N. Zhao, et al., Improved tumor targeting and longer retention time of NIR fluorescent probes using bioorthogonal chemistry, Theranostics 7 (15) (2017) 3794–3802.
[141] S.H. Kong, Y.W. Noh, Y.S. Suh, et al., Evaluation of the novel near-infrared fluorescence tracers pullulan polymer nanogel and indocyanine green/γ-glutamic acid complex for sentinel lymph node navigation surgery in large animal models, Gastric Cancer 18 (1) (2015) 55–64.
[142] M. Al-Taher, M. Barberio, E. Felli, et al., Simultaneous multipurpose fluorescence imaging with IRDye® 800BK during laparoscopic surgery, Surg. Endosc. 35 (8) (2021) 4840–4848.
[143] H. Tsujimoto, Y. Morimoto, R. Takahata, et al., Theranostic photosensitive nanoparticles for lymph node metastasis of gastric cancer, Ann. Surg Oncol. 22 (Suppl 3) (2015) S923–S928.
[144] M. Diana, E. Robinet, Y.Y. Liu, et al., Confocal imaging and tissue-specific fluorescent probes for real-time in vivo immunohistochemistry. Proof of the concept in a gastric lymph node metastasis model, Ann. Surg Oncol. 23 (Suppl 5) (2016) 567–573.
[145] J. Yang, J. Huang, Y. Yang, et al., Confocal laser endoscopy in the diagnosis for abdominal lymph node metastasis of gastric cancer, Int. J. Clin. Exp. Med. 8 (6) (2015) 8905–8915.